Summary of Fisheries Sonar Field Evaluations in the southern Strait of Georgia, Sept. 1998

by Mark V. Trevorrow and David M. Farmer

Acoustical Oceanography,
Institute of Ocean Sciences,
Sidney, B.C. Canada

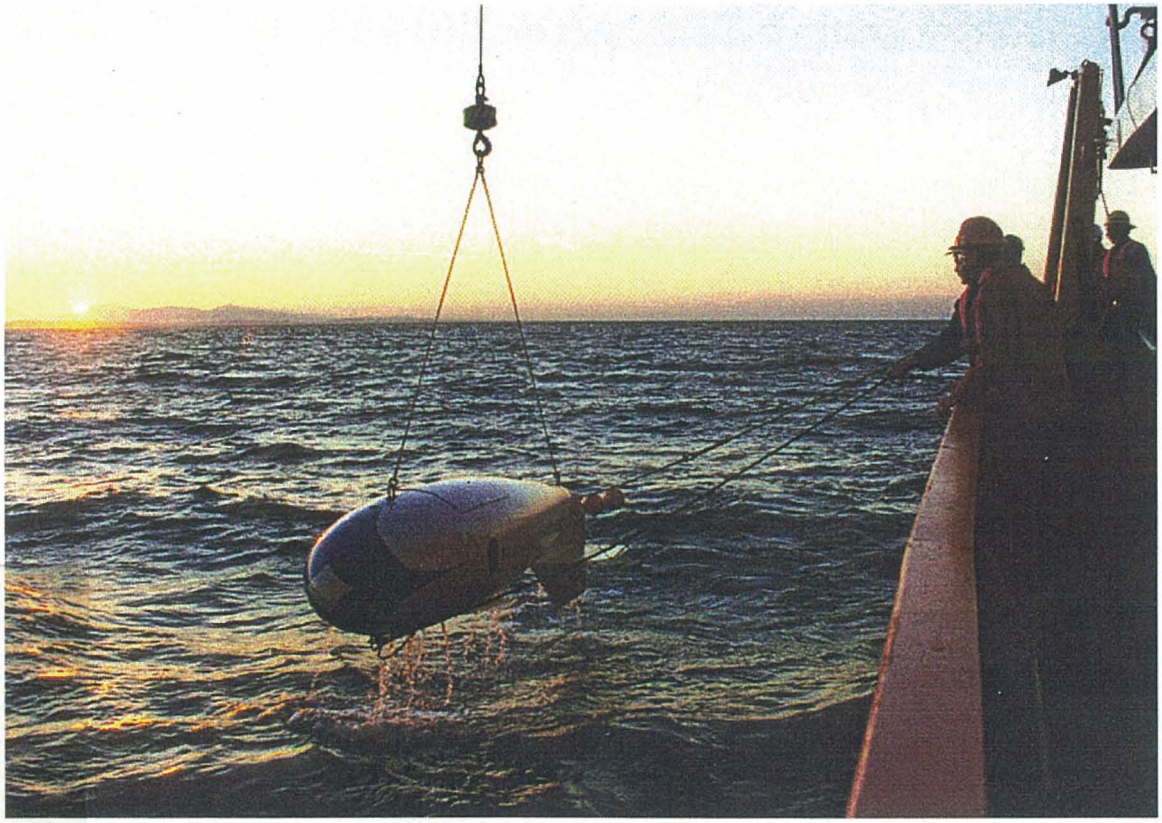

Towfish Recovery at Sunset, Sept. 9th 1998 in the Strait of Georgia

Summary:

This report presents an overview of results from a second sea-trial of a prototype intermediate range fisheries sonar (IRFS), which was conducted from the *CCGS Vector* from Sept. 8th to 16th, 1998 in the southern Strait of Georgia near Vancouver, B.C. The primary objective was to assess the feasibility of a towed side-looking sonar for detection of migratory salmon at longer ranges. This location near the mouth of the Fraser River was again chosen because of the large concentrations of late-run Sockeye salmon expected to congregate in this area prior to their migration into the river, and because of significant independent fisheries information available on these Sockeye. During the sea-trials the 12kHz sonar array was towed at a speed near 4 knots at a nominal depth of 35 m. During towing operations typically lasting 6 to 10 hours per day, pulse repetition periods of 6.6 to 10 s were used, allowing horizontal ranging from 4.7 to 7.2 km. Before the Sept. 1998 sea-trials the IRFS system was modified for *in situ* digitization with digital data telemetry, and for improved horizontal sonar directivity using epoxy foam backing materials. For comparison purposes, a 100kHz echo-sounder was operated from the *Vector*, a 120kHz split-beam echo-sounder was operated from a small survey launch, and a 200kHz moored inverted echo-sounder was deployed. Additionally, the performance of a towed 330kHz vertical sector scanning sonar was evaluated for detection of near-surface fish. Furthermore, a series of side-by-side comparisons with net-trawls conducted by the *CCGS W.E. Ricker* were performed on Sept. 16th.

Overall, the IRFS and all the echo-sounders were not successful at detecting adult salmon in this region, in distinct contrast to results from the Aug. 1997 trials. The reason for this was that these late-run Sockeye began their migration on or about Sept. 10th, roughly 10 days earlier than historical expectations. By the time the IRFS trials began the salmon had already moved into shallow, near-shore areas near Sandheads and Canoe Pass and thus were difficult to detect using these sonar methods. This was confirmed by Pacific Salmon Commission riverine escapement data and *Ricker* net-trawl results. Also, acoustic propagation calculations using a ray-tracing approach based on measured water properties and bathymetry showed that a near-surface shadow zone beyond 2000 m range would obscure fish targets in the near-shore regions. Herring schools were consistently observed with both the IRFS and echo-sounders in areas on the western slopes of Sturgeon and Roberts Banks. Finally, some evidence for vessel-avoidance reactions by the fish was found with the 330kHz scanning sonar and the three echo-sounders. The report concludes with recommendations for further engineering improvements and possible locations for more field trials.

Mark V. Trevorrow:
Acoustical Oceanography, Institute of Ocean Sciences, 9860 W. Saanich Rd., Sidney, B.C. Canada V8L 4B2, tel (250) 363-6448, fax -6798, TrevorrowM@dfo-mpo.gc.ca

David M. Farmer:
Acoustical Oceanography, Institute of Ocean Sciences, 9860 W. Saanich Rd., Sidney, B.C. Canada V8L 4B2, tel (250) 363-6591, fax -6798, FarmerD@dfo-mpo.gc.ca

1. Introduction and Motivation:

A challenge to fishery surveys is the acquisition of data over an area sufficient to allow accurate abundance estimates. Vertical echo-sounders and echo-integration techniques are well-established, but the usefulness of such measurements is often compromised by limited spatial coverage within a survey area and the consequent need for statistical compensation. Surveys of shallow-water or epi-pelagic stocks are further limited by a small sampling volume beneath the ship and avoidance behaviour by the fish. In contrast, side-looking sonars have the potential for fish detection to horizontal ranges of order several kilometers, even in shallow waters, providing spatial coverage several orders of magnitude greater than for conventional echo-sounders or net trawls. This work reports an evaluation of the feasibility and limitations of this side-looking sonar concept for fishery surveys.

Fish have been detected at horizontal ranges up to 65 km using high-power, low-frequency sonars (Weston & Revie 1971, 1989; Rusby et al. 1973; Revie et al. 1990; Weston & Andrews 1990). The powerful sonars used in these earlier studies might have restricted application given current concerns about effects of noise on marine mammals. More recently, fish detection has been demonstrated using high-frequency (>50 kHz) horizontally-oriented sonars at ranges up to a few hundred meters (e.g. Hewitt et al. 1976; Gaudet 1990; Misund et al. 1995; Tarbox & Thorne 1996; Trevorrow 1997; Trevorrow & Claytor 1998). In this work we explore the feasibility of 12 kHz sidescan sonars for fish detection over ranges of 1 to 7 km, which we identify as of intermediate range, lying between ranges accessible to the high (~100 kHz) and low (~1 kHz) frequency systems described previously. This particular set of field evaluations builds upon promising results generated in Aug. 1997 with an earlier version of this 12 kHz sonar (reported in Farmer et al. 1999) in this same region. In 1998 a variety of additional sonar systems were deployed in an effort to provide better ground-truth information on the abundance and distribution of salmon and other fish.

Complications arise with the side-looking geometry due to boundary scattering, refraction and multiple reflections. In contrast to vertically oriented sonar applications, acoustic propagation effects become important, necessitating measurement of the bathymetry and sound speed distribution, combined with appropriate propagation analysis. Furthermore, at frequencies significantly higher than the swim bladder resonance the back-scatter cross-section of a fish at horizontal incidence is sensitive to fish orientation relative to the acoustic beam. Although these acoustic features complicate interpretations of data from horizontally oriented fisheries sonars, improved understanding appears likely to lead to techniques that can add significantly to the more established vertical sounding methods.

The location (see Figure 1) and timing of these sea trials were chosen to coincide with the large Adams River Sockeye salmon (*Oncorhynchus nerka*) run known to enter the mouth of the Fraser River in September. Considerable independent sampling of this salmon run is conducted by both DFO and the Pacific Salmon Commission (PSC), which serves as an excellent source of comparison data. Additionally, during summer the southern Strait of Georgia has a refractive sound channel at 20-60 m, formed beneath the warmer, fresher Fraser River outflow.

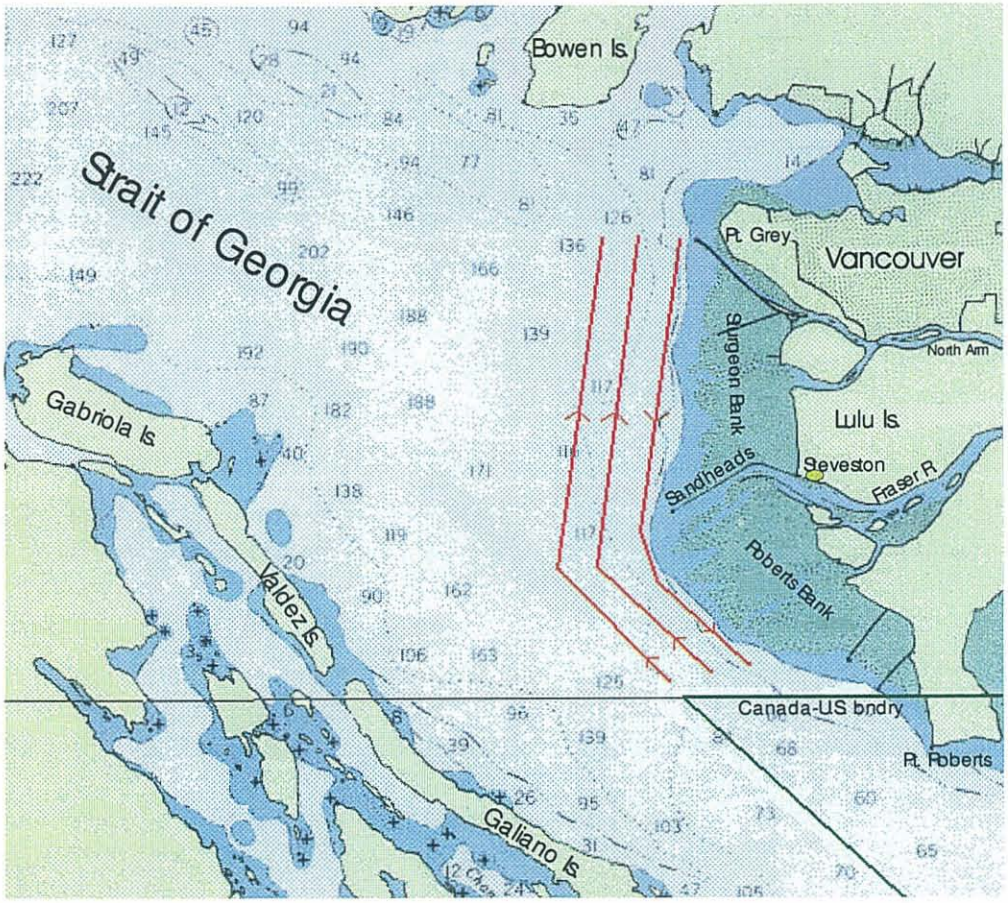

Figure 1: Map of the southern Strait of Georgia near Vancouver, B.C., showing in red the approximate IRFS tow paths offshore of Sturgeon and Roberts Banks.

2. Description of Instrumentation:

Significant modifications to the original IRFS system were implemented prior to the Sept. 1998 field trials. An overview diagram of the improved system is shown in Figure 2.1. The two major system improvements were the implementation of *in situ* digitization with digital data telemetry up the tow cable, and improved transducer vertical beam directionality using syntactic foam backings. Both of these improvements were implemented and tested during the summer of 1998.

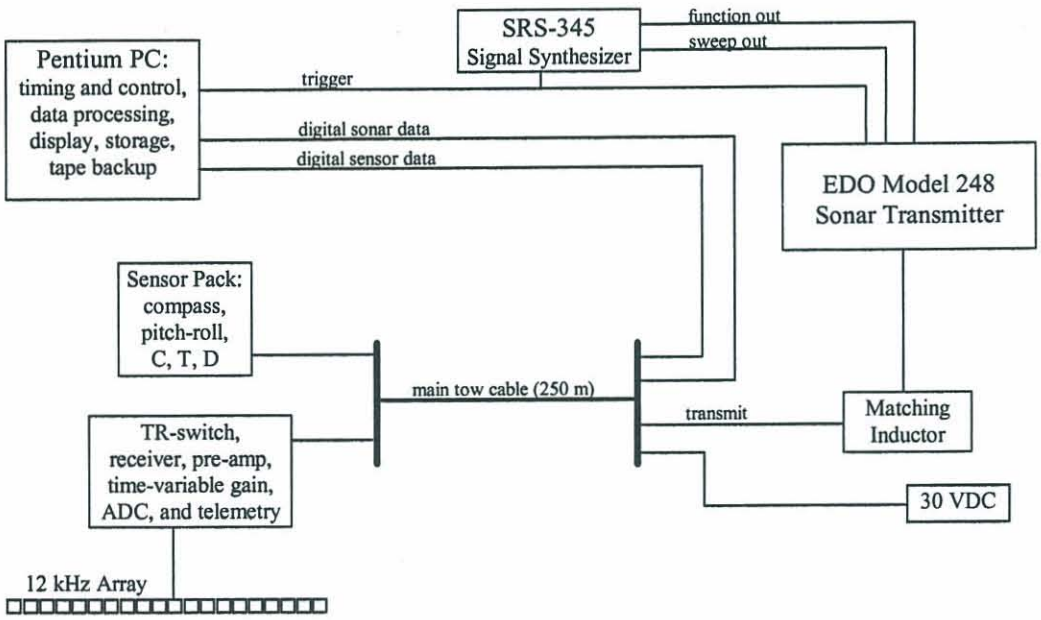

Figure 2.1: Block diagram of the 1998 digital IRFS components and connections.

With the exception of the in situ digitization and telemetry systems, the IRFS electronics and computer system was the same as used in the Aug. 1997 field trials. The heart of the system was a 40-element, 2.5 m aperture linear transducer array operating at 12 kHz center-frequency. In the horizontal plane the array had a measured beam-width (total angle to -3 dB) of 2.8°. A 100 or 200 ms duration by 1600 Hz synthesized FM sweep pulse was fed to an EDO model 248 transmitter, which was used to deliver up to 2 kW (electrical) to the transducer array. This resulted in a forward (on-axis) transmit source level of 218 dB re 1 μPa at 1 m. All the analog receiver electronics were housed within the sonar towfish. This package consisted of a transmit-receive (TR) switch, a pulse detector/trigger circuit, and a bandpass-filter pre-amplifier circuit with a combination of fixed and time-varying gain (TVG). A 20 dB fixed pre-amplifier stage was provided. A microprocessor was used to generate the TVG control voltage, the form of which could be modified on command from the surface PC. At the leading edge of the transmit pulse the pulse detector triggered the microprocessor to begin the TVG cycle. The TVG curve had a lockout during the transmit pulse (e.g. the first 200 ms), followed by a linear increase of 8.0 dB per second up to a user controller duration (e.g. 8 s), then constant until the next trigger. Overall the TVG was limited to a maximum of 80 dB.

In order to reduce the effects of extraneous noise in the tow-cable, an *in situ* digitization capability was implemented. This was accomplished using a 2-channel CODEC chip integrated within an Analog Devices 21061 digital signal processing (DSP) card. During data acquisition, samples were produced at 5333.33 samples per second, which was two and one-quarter cycles of the chirp 12.0 kHz center frequency. Coherent sampling was accomplished by driving the CODEC sampling with an external 48.0 kHz clock sent down the tow-cable. The CODEC chip also provided additional fixed gain up to 22.5 dB, controlled by commands from the surface PC. The DSP relayed the digital samples to a RS-485 format high-speed serial modem for transmission up the tow-cable. The surface PC decoded this serial data stream and performed real-time complex correlation with the

transmit pulse template (via FFTs) to achieve up to 25 dB processing gain. The surface PC also performed data display, binary data storage, and a graphic user interface for system control using a National Instruments LabWindows programming environment. The control interface also interrogated a towfish attitude (compass, pitch-roll) and conductivity-temperature-depth (CTD) sensor package, communicating via RS-485 serial protocol.

Extensive pre-trial bench testing and calibration of the system electronics was performed. The lowest electronic noise level in the system was -100 dB (re correlation units), corresponding to an equivalent input voltage of 0.19 mV rms. The ADC maximum input of 6.0 V (peak-to-peak) corresponded to a correlated output of -19.4 dB, producing an overall systemic dynamic range of 81 dB. The effective pulse width after correlation processing was measured at 0.8 m (theoretically should be ½·c/1600 Hz = 0.46 m), with greater than 60 dB side-lobe rejection. Combining the acoustic calibrations of the 40-element array performed by the manufacturer (EDO/Western) with the measured electronic characteristics, an overall system calibration could be derived.

The 40-element array, TVG pre-amp and digitizer electronics, and attitude/CTD sensor package were all mounted within a 5.4 m long streamlined tow-body (same as Aug. 1997). The 12 kHz array was mounted on the starboard side of the tow-body, with its main axis horizontal and oriented 4.7° aft of perpendicular to the tow-body axis. The tow-body was connected to the ship-board systems via a 250 m long, 12-conductor electro-mechanical tow-cable. A 360 kg depressor weight was attached to the cable approximately 20 m ahead of the tow-body. The tow-body was deployed to a 35 m (nominal) depth from the starboard-quarter A-frame on the *CCGS Vector*. Cable strumming during towing operations was minimized by loose wrappings of heavy string around the outside of the cable. The tow-body itself was approximately neutrally buoyant in seawater.

To improve the forward directivity and vertical beam-pattern of the transducer array, syntactic foam absorbing-reflecting material was mounted on the back and top and bottom sides along the entire 2.5 m length of the array. The final configuration, arrived after a series of lab tests with a single element, used 102 mm thick syntactic foam rated for 50 m operating depth. The foam had a measured density and sound speed of 240 kg/m^3 and 1100 m/s respectively, yielding a 12 kHz reflectivity coefficient of 1.4. The top and bottom sides extended slightly forward of the transducer front face. The improvement in measured transducer directivity is shown in Figure 2.2 (the green curve corresponds to the syntactic foam configuration actually used in the sea trials). Quantitatively, the bare transducer had a beam-width (total angle to -3dB) of 122°, a front-to-back ratio of only 6 dB, and a significant side-lobe at 110° (note that beam-patterns are symmetric about the main axis). With the syntactic foam backing and 127 mm sides, the total beam-width was reduced to roughly 60°, with a front-to-back ratio of 39 dB and minimal sidelobes. Since the effects on the beam-pattern are significantly stronger than indicated by the reflectivity coefficient alone, it can be concluded that the dominant action of the syntactic foam is as an acoustic absorber.

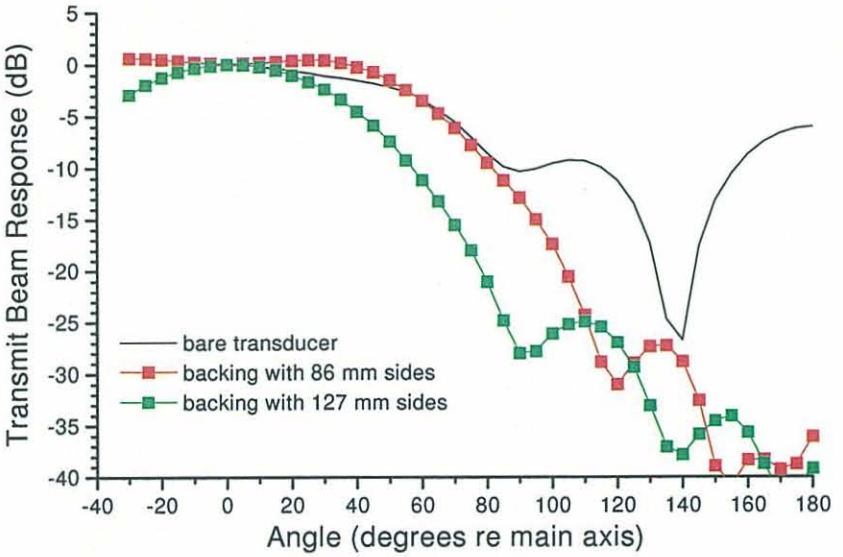

Figure 2.2: Effects of syntactic foam backing material on transducer directivity.

For comparison purposes, several higher frequency acoustic systems were employed during the Sept. 1998 sea-trials. During all IRFS towing operations, a 100 kHz vertical echo-sounder was operated from the *CCGS Vector* (same as in Aug. 1997). This system was based around a BioSonics model 101 transceiver connected to a hull-mounted transducer on the *Vector*. This transducer had a conical beam with width (total angle to -3 dB) of 3.0°. The echo-sounder was operated with a pulse length of 0.4 ms (30 cm acoustic resolution), pulse repetition period of 0.5 s, and a 20log[r] TVG. The echo amplitude output was digitized and stored using a PC-based data acquisition system. The echo-sounder data was sampled at 12 kHz (6.2 cm sampling resolution) with 16-bit ADC resolution to a maximum depth of 150 m. The ship's position, speed, and heading were continuously monitored with a differential GPS system. Combining the manufacturer's acoustic calibration of the transducer with measured system characteristics, a rough acoustic calibration is available for this echo-sounder.

For mobile echo-sounder surveys, a Simrad EK-500 split-beam was deployed on a small survey launch (the *Grebe*, shown in Figure 2.3). This system was contributed by I. McQuinn of the Institute Maurice Lamontagne, who traveled to IOS to join the first week of the sea trials. Generally, the *Grebe* performed simultaneous near-shore surveys while the *Vector* towed the IRFS northbound, looking towards shore and the *Grebe* survey area. This fully calibrated EK-500 utilized a 7.1° beam, 120 kHz transducer, operated with a pulse length of 0.3 ms and a pulse repetition rate of 2 Hz. The split-beam capability allowed the extraction of single fish target range, alongship, and athwartship angles, thus enabling correction for beam-pattern effects and estimation of the true fish target strength. Single-target, bottom tracking, and volumetric scattering strength data were logged with an on-board PC. Echo-sounder control, data acquisition, and display were performed by the newly developed CH1 program developed at IML. Position, speed, and heading information from a differential GPS were fed into the Simrad system for inclusion with the echo-sounder data. Owing to weather and logistical constraints, the *Grebe* was only operated on Sept. 9th through 12th.

Figure 2.3: Survey launch *Grebe* used for supplemental EK-500 echo-sounder surveys. The 120 kHz transducer was mounted on a para-vane (not visible in photo) beneath the starboard side support frame.

Feasibility tests of a towed sidescan sonar for near-surface fish detection were performed on Sept. 14th, 15th, and 16th. This system was built around a 330 kHz Imagenex model 858 imaging sonar (denoted the IMX sidescan), and was used in both conventional sidescan and vertically steerable configurations. The goal of these tests were to provide near-surface fish depth distributions and to assess any possible vessel-avoidance behaviour by the fish. The 330 kHz sidescan beam was roughly fan-shaped (1.8° by 18°). The sidescan transmitted a 0.1 ms pulse at a rate of 5 Hz, sampling with 5 cm resolution to 100 m maximum range. The sidescan used a $20\log[r] + 0.1 \cdot r$ TVG pre-amplifier. Data was displayed and logged in a ship-board processor. The sidescan was integrated within a 1.2 m long towfish (see Figure 2.4), which also supported pitch, roll, compass, and depth sensors. This towfish was deployed from the port quarter of the *Vector* at a nominal depth of 18 m. In the conventional sidescan mode the beam was fixed 90° to port (away from the ship and wake) with the wide axis oriented vertically. In the vertical scanning mode the wide beam axis was oriented parallel with the tow-direction and the beam scanned over a 30° vertical sector in 1.2° steps, requiring 5.0 s to complete a scan. The 30° sector was oriented horizontally to port so that over some portions of the scan the beam intersected the surface. Along with the towfish depth and roll angle, the fish target range and azimuthal angle allowed extraction of the horizontal range and depth of the individual fish targets. This system had been acoustically calibrated using the backscatter from tungsten-carbide target spheres.

Figure 2.4: 330 kHz steerable sidescan towfish during deployment from the stern of the CCGS Vector.

For more complete temporal coverage at a single location, a 200 kHz moored inverted echo-sounder (WASP) was deployed 48 m below the surface in roughly 75 m water depth approximately 3.5 km north of Sandheads (N49° 08.33′, W123° 18.16′). Figure 2.5 shows the WASP instrument at the surface during deployment on Sept. 8th. WASP was completely self-contained, with echo-sounder electronics, internal batteries, and data storage hard-drives housed within a 20 cm diameter by 90 cm long pressure case. The 200 kHz transducer had a conical beam with 5° total angle (to -3 dB). WASP was programmed for continuous operation with a ping rate of 1 Hz, a pulse length of 0.5 ms, averaged over a vertical bin size of 21.5 cm, with 8-bit sampling resolution and no TVG. The recorded data spanned the surface to roughly 33 m depth. The instrument operated continuously from its deployment at 1805h on Sept. 8th until recovery at 1420h on Sept. 16th (all times PDT, UTC - 7h). Similar to the sidescan, WASP had been acoustically calibrated using the backscatter from target spheres. In addition to the volume scattering strength data which are dominated by zooplankton populations, WASP provided measurements of the range to the surface, which was consistent with tidal information. During windy periods sufficient to create surface whitecapping, WASP also observed volumetric scattering due to near-surface bubble plumes.

In order to characterize the acoustic propagation conditions, occasional CTD profiles were conducted from the CCGS Vector. The CTD casts utilized a SeaBird Electronics SBE-911plus, with dual temperature and conductivity sensors. The resulting water temperature and salinity vs. depth data were then used to calculate sound speed profiles (among other oceanographic uses). The time and location of these CTD casts is listed in Appendix 2.

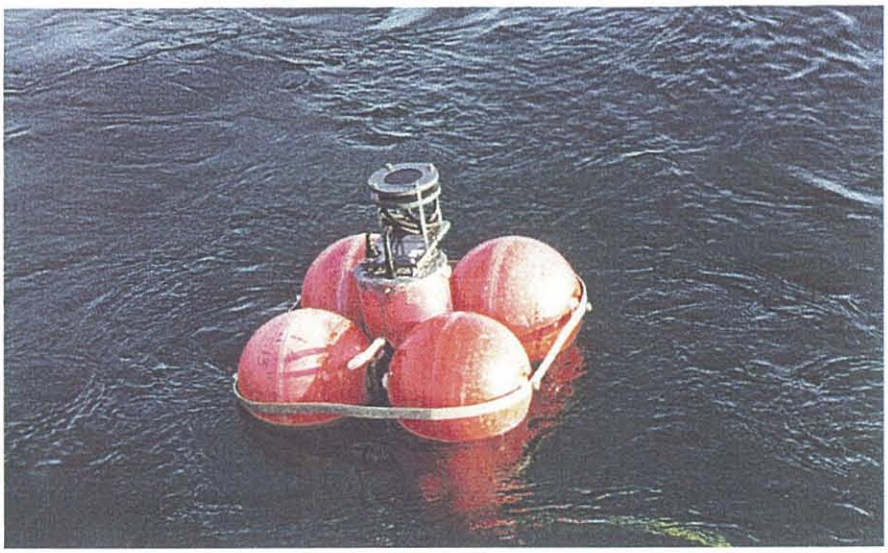

Figure 2.5: Self-contained WASP instrument with 4 floatation spheres. The 200 kHz transducer is the black disk within the topmost support bracket.

3. Supplementary Environmental and Fishery Data:

The southern Strait of Georgia was again chosen as an ideal location for the IRFS sea trials because of the known, consistent presence of migratory adult salmonids, with good quality, independent fishery information on those fish, and favorable acoustic propagation conditions. A ubiquitous feature of the southern Strait of Georgia in the summer and early fall is the appearance of a sub-surface refractive sound channel. Figure 3.1 shows a typical CTD and resulting sound speed profile from this area. The figure shows a distinct surface layer, 5 to 10 m deep, resulting from the warmer, fresh water outflow from the Fraser River. The waters from 10 to 40 m depth were characterized by strong temperature and salinity gradients as tides and wind-wave action mixed the Fraser River waters with deeper, bulk waters of the Strait of Georgia. The result for acoustic propagation was the formation of a sound speed minimum near 40 m depth, with strong downward refraction in the surface layer and weaker upward-refracting conditions below. The strong downward refraction near the surface had the positive effect of minimizing the backscattered interference from surface waves, breaking wave-induced bubbles, and vessel wakes. A negative implication of this downward refracting surface layer is the occurrence of significant proportions of the Sockeye salmon population (perhaps in excess of 80%) within the upper 20 m, where they are undetectable with the IRFS.

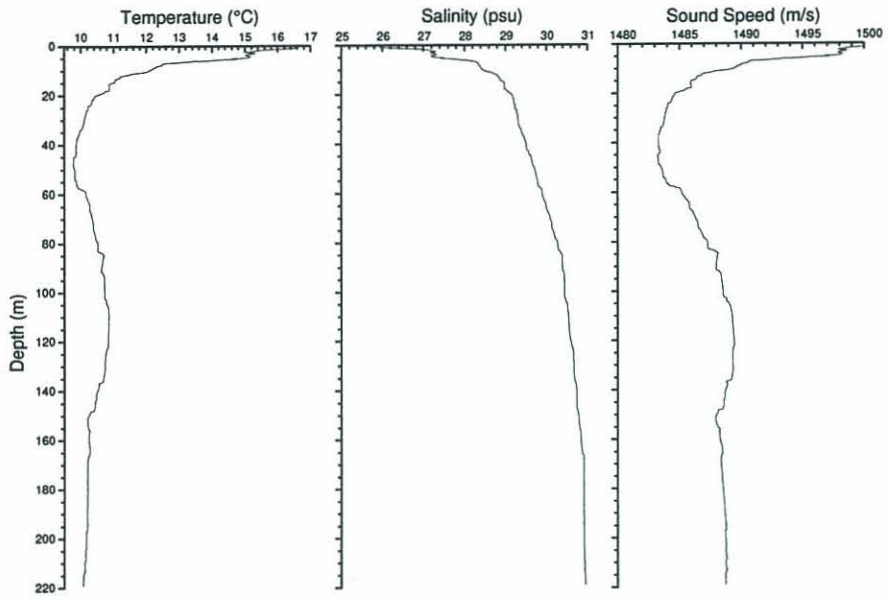

Figure 3.1: Typical temperature, salinity, and sound speed profiles taken from the south-eastern Strait of Georgia (data taken 1512PDT, Sept. 12, 1998 approx. 2 miles West of Vancouver Airport).

The IRFS operations took place just at the beginning of the *Late* or *Adams River* Sockeye run, as shown in Figure 3.2. The total escapement near Mission, B.C. was estimated from echo-soundings taken with a boat continuously transecting the river. Additionally, test fisheries (gillnets) were conducted on alternate days near Steveston and Whonnock, B.C. to identify species and produce a relative catch per unit effort (CPUE) index of abundance. The daily estimates from Mission were back-propagated by 48 hours to compare with the IRFS and test fishery operations. During Sept. the dominant species was Sockeye (*Oncorhynchus nerka*), averaging between 85% and 99% of the test catches. The remainder of the test catches were composed of a few Chinook (*O. tshawytscha*), Coho (*O. kisutch*), and Chum (*O. keta*) salmon. The mean weight of the Sockeye was 2.83 kg. The total estimated escapement of Fraser Sockeye for the month of September was 2.8 million past the Mission, B.C. site, averaging 157 thousand per day with a high of 536 thousand on Sept. 14th. There were no commercial fishery openings during September in this area. The IRFS sea-trials were scheduled to take advantage of the fact that the Adams River Sockeye congregate in the southern Strait of Georgia for a 2 to 3 week period prior to migrating up the river, historically with the run maximum near Sept. 20th every year. For reasons only known to the salmon, they began their migration on approximately Sept. 11th. Large numbers of Sockeye were visually observed at the surface and jumping out of the water in the near-shore areas near Sandheads and in the lower Fraser River on Sept. 9th through 14th. Unfortunately, this early migration and observed presence in the near-surface waters near Sandheads made the Sockeye largely unavailable for detection by the IRFS, due to the downward-refracting acoustic propagation conditions (described in section 4).

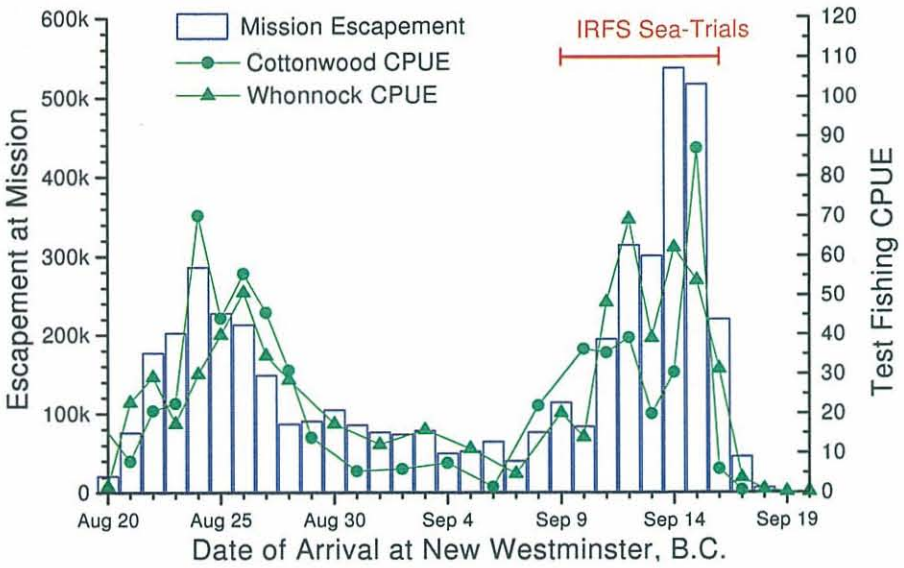

Figure 3.2: Total Sockeye salmon escapement at Mission, B.C. and test-fishery (gillnet) catch per unit effort for Aug. 20th to Sept.19th, 1998. Data from Pacific Salmon Commission courtesy of J. Woodey.

On Sept. 16th a series of five side-by-side comparisons with net trawls performed by the *CCGS W.E. Ricker* were conducted in the area from Canoe Pass to Pt. Grey (see Figure 3.3). This collaboration took advantage of an existing DFO program for surveying salmonids in the Strait of Georgia. The standard trawls on the *Ricker* utilized a 12 m deep by 36 m wide rope trawl net, towed for 30 minute duration at speeds near 5 knots. The depth of the net could be controlled from the surface to 60 m. The *Vector* was directed to steam a parallel course to the *Ricker* trawls at a distance between 1 and 2 km to seaward of the *Ricker*. During these runs the IRFS, IMX sidescan, and 100kHz echo-sounder on the *Vector* were all operated. Biological information such as species, sex, length, weight, scales, and otoliths were collected from the fish recovered. The trawl results from 6 separate sets in the southern Strait of Georgia are summarized in Table 1. Only 1 Sockeye and only 6 other adult salmon were caught during the 6 trawl sets, in spite of the large numbers of Sockeye known to be moving into the Fraser River at this time (see Figure 3.2). Three of the trawl sets did not catch any adult salmon. A plausible explanation for this is that by Sept 16th the Sockeye had dominantly moved into the shallows near the Fraser River mouth and were thus unreachable with the *Ricker* trawls. It is interesting to note the presence of several larger (75 to 93 cm length) Chinook and Chum salmon caught at depths from the surface to 30 m. Owing to their larger acoustic target strength and greater depth of occurrence it is likely that these salmon would be detectable with the IRFS. A significant number of herring (*Clupea harengus pallasi*) were collected, especially in the trawls just south and north of the Sandheads area. It is probable that trawl set 84 captured a herring school. When schooling, herring will have sufficient acoustic backscatter strength to be visible with the IRFS. Also found were a significant number of juvenile salmon (denoted *Jacks* in Table 1 as a generic term covering all species). These were similar in size to the adult herring, although since they were not schooling fish it was unlikely that they would be observed with the IRFS.

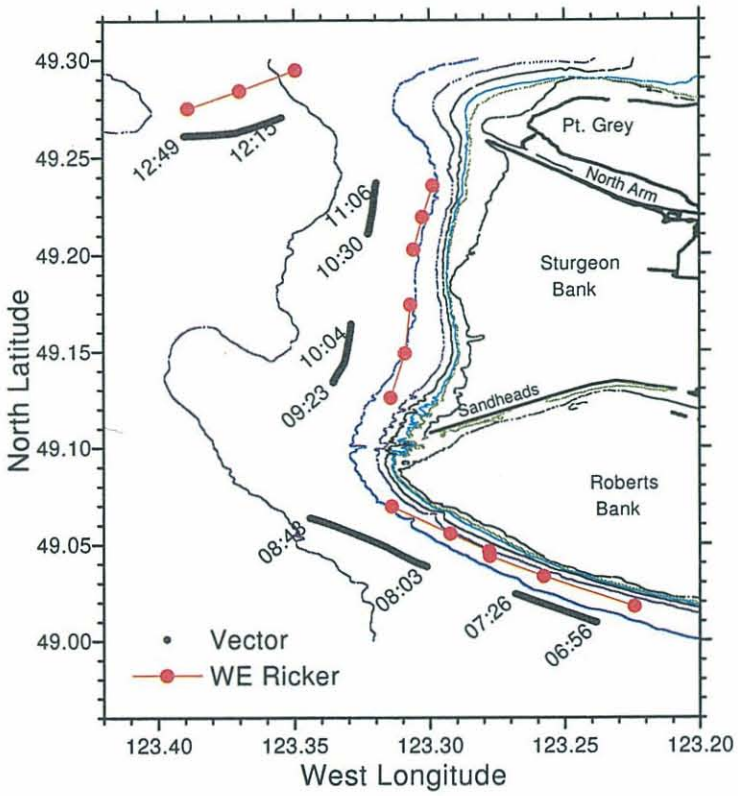

Figure 3.3: Paths of *CCGS Vector* and *W.E. Ricker* during acoustic vs. trawl comparisons on Sept. 16th.

Table 1: Trawl results from the CCGS W.E. Ricker, Sept. 16th, 1998 in the southern Strait of Georgia. Data courtesy R. Sweeting of the Pacific Biological Station, Nanaimo.

Set	Start Time	Start Location	Distance, Heading	Trawl Depth	Adult Salmon, mean length	Other Fish
81	06:58	N49° 01.05′ W123° 13.45′	2.65 nm, 307°	surface	1 Sockeye 58.4cm 1 Chum 81.5cm 1 Chinook 93.0cm	52 herring 9 jacks 22cm
82	08:04	N49° 02.77′ W123° 16.68′	1.99 nm, 315°	15 m	2 Chum 75.5 cm	287 herring 1 hake 13 jacks 22cm
83	09:28	N49° 07.52′ W123° 18.87′	2.93 nm, 006°	surface	none	3 jacks 16cm
84	10:33	N49° 12.13′ W123° 18.35′	1.99 nm, 008°	30 m	1 Chinook 85.8cm 1 Chum 72.8cm	5560 herring 4 jacks 22cm
84	12:11	N49° 17.66′ W123° 20.95′	1.90 nm, 230°	60 m	none	199 herring 5 jacks 20cm
86	13:10	N49° 15.93′ W123° 25.40′	2.58 nm, 230°	surface	none	10 herring 212 jacks 19cm

4. Towed 12kHz Sonar Results:

As in 1997, towing operations were conducted in a region bounded by Point Grey on the North and the Canada-U.S. border on the South, and West to approximately 4 miles offshore of Sturgeon and Roberts Banks. The starboard look direction of the IRFS required the towing operations to follow a clockwise circuit: southbound along the eastern shore and northbound out in the center of the southern Strait. The southbound tracks were chosen to be close to shore but maintaining a minimum water depth of 80 m. Also, this region contains the busy north- and south-bound traffic lanes for the Port of Vancouver, as well as a concentration of vessel traffic to/from the Fraser River at Sandheads. This imposed a constraint that northbound tows could only run within the traffic separation zone at 2 nautical miles offshore or outside (west of) the south-bound vessel traffic lane at 4 miles offshore. The majority of data was collected during Northbound tows in the vessel traffic separation zone roughly 2 miles offshore of Roberts and Sturgeon banks. Appendix 1 gives a detailed timetable of the cruise operations.

Typical towing operations began near 0800h each day at one end of the tow tracks shown in Figure 1. CTD casts to within 5 m of the seabed were conducted at the beginning and end of each track, and along each track at turning points or convenient stopping times. The towfish was deployed to depths of 35 to 40 m, and the ship was directed to steam at a constant speed of 3.5 to 4 knots (relative to the water) along a fixed heading. In practice, maintaining a strictly constant speed and heading was difficult due to wind, tides, and the need to avoid other vessel traffic. During the northbound tows 2 miles offshore of Roberts and Sturgeon Banks, the IRFS was operated with a 100 ms pulse and ping intervals of 5.71 to 6.67 s, sampling to maximum ranges of 4.2 to 4.8 km which was sufficient to reach the edge of shallow banks. Southbound runs near shore used a 10 s ping interval and a 200 ms pulse to sample ranges up to 7.2 km.

In contrast to the Aug. 1997 results, in general the IRFS did not observe many individual fish tracks. However, larger school-like objects were observed, particularly in the area between Sandheads and North Arm. Figure 4.1 shows a typical example of these schools, which can be contrasted with a few individual fish tracks (e.g. near 2500m, ping 280). These schools were clearly detectable because the maximum intensity of the schools was at least 10 dB above the background reverberation. The typical dimensions were 50 to 100 m in thickness with duration in the beam of up to 300 s (5 minutes). Based on the fact that the *W.E. Ricker* trawls returned large numbers of herring in this region, and that herring schools were observed in echo-sounder data (to be discussed in later chapters), it is most likely that these objects were herring schools. If the identity and size of the fish in these schools could be established, it is conceivable to use the integrated echo intensity to estimate the biomass in these schools. It is also possible that these objects were aggregations of sockeye salmon, however this would imply there are distinct behavioural differences between summer run (which do not school, as observed in Aug. 1997) and these Adams River run Sockeye. These schools were generally found within 1 km of the *acoustic shore*, which is defined by a strong increase in backscatter level when the 20 to 60 m sound channel intercepts the edge of Sturgeon and Roberts Bank. The IRFS was not able to detect fish within or beyond this *acoustic shore* region. A small portion of the *acoustic shore* near the Sandheads area is visible in the bottom

left-hand corner of Figure 4.1. Thus, these schools were most likely located at depths of 20 to 60 m overlying the steep slopes on the western fringes of Sturgeon Bank. In the first 1000 to 1500 m (not shown) of the IRFS data, fish detection was difficult as the data was generally contaminated by higher levels of seabed backscattering. Also, targets located in the first 1 km appeared for only 1 or 2 pings, making them difficult to recognize relative to the background reverberation.

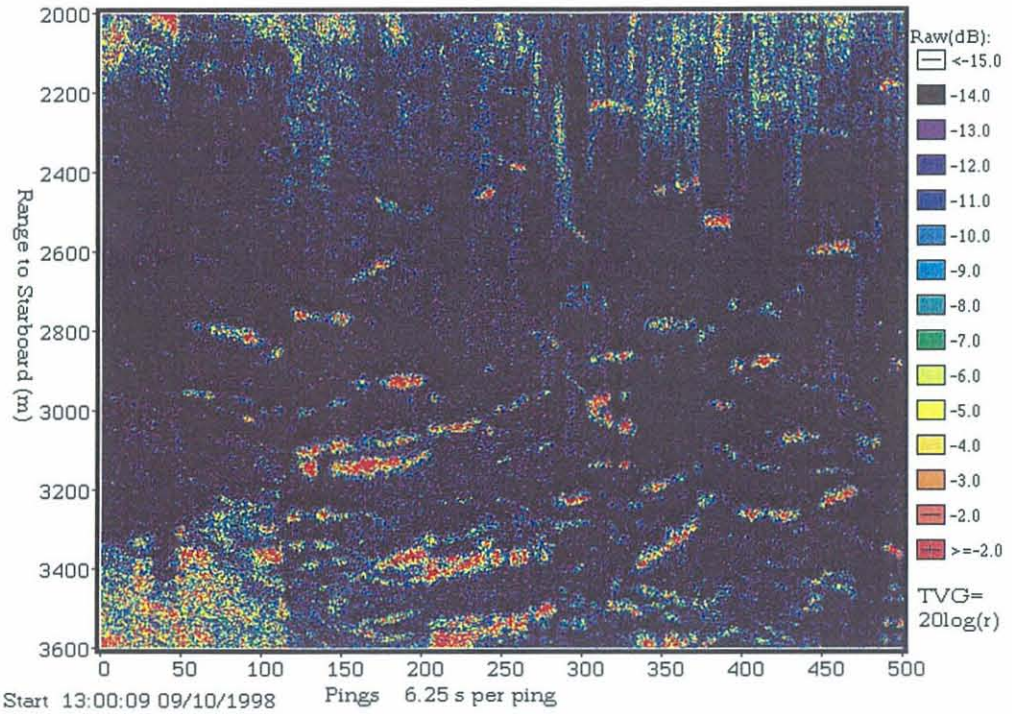

Figure 4.1: IRFS range vs. time raw intensity echogram starting 1300h Sept. 10th. Total duration is 52 min., 5 s. IRFS was towed northbound at 3.7 km offshore of Sturgeon Bank just north of Sandheads. Echo intensities are raw correlation units in dB, corrected to a 20log[r] variation.

For more quantitative analysis, the most straight-forward (albeit time-consuming) method for extracting the fish targets from the IRFS data was to manually select targets from images such as Fig. 4.1. Information such as target range, time, width, duration, area, and intensity was extracted for each target. Then individual fish or school target locations can be calculated from the measured range and time to each target within the IRFS data, the position and heading of the ship, and the towed-body orientation. A map of the detected targets relative to the bottom bathymetry can then be created, with an example shown in Figure 4.2 for the northbound run on Sept. 11th. The figure also shows the path of the survey launch Grebe which conducted simultaneous near-shore surveys with a split-beam echo-sounder on the edge of Roberts and Sturgeon Banks. Excluding the first 1 km of data (where fish were not generally detectable), the total area covered by this 5.5-hour northbound tow was approximately 30 x 3.5 km, or 105 km^2. Over this area 125 fish targets, mostly schools, were observed. Overall, the detected fish targets were clustered along the 100 m contour, with somewhat greater densities to the South and North of Sandheads.

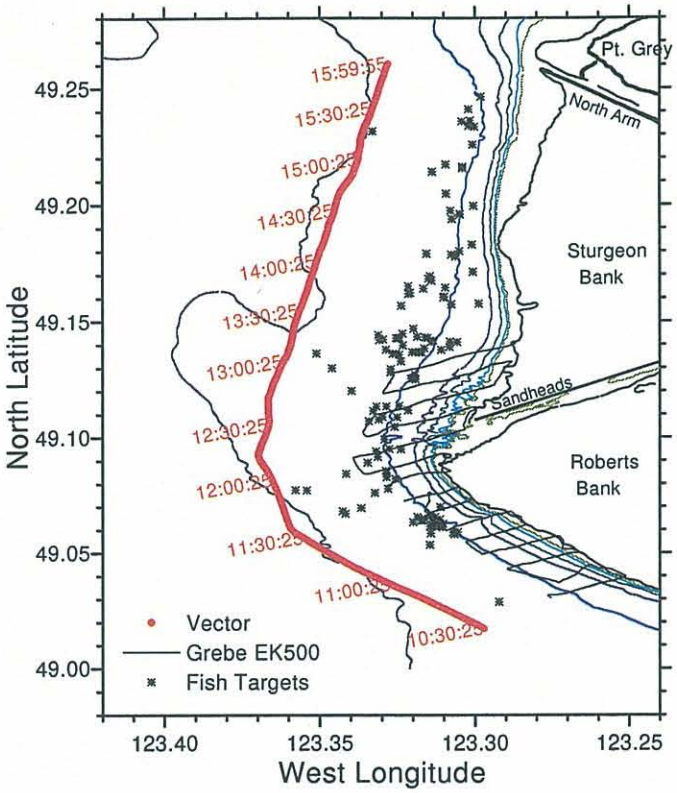

Figure 4.2: Map of Sandheads area showing locations of Vector tow-path, Grebe split-beam echo-sounder surveys, and detected fish targets (mostly schools) on Sept. 11th, 1998. Contours are shoreline, 2m, 10m, 20m, 40m, 60m, 100m, and 200m.

The acoustic propagation conditions determine the effectiveness and effective sampling volume of this side-looking sonar. To better understand the effects of acoustic propagation, a ray-tracing code due to Bowlin et al. (1992) was used to calculate sound pressure level as a function of range and depth for a given source depth, bathymetry, sound speed profile, and sediment conditions. Eigenrays connecting the source and range-depth matrix of potential fish target locations were calculated for rays launched within ±30° of horizontal. The resulting intensities were summed incoherently on a grid with spacing 20 m range by 1.5 m depth. Figure 4.3 shows an example for propagation onshore at a distance of 3.5 km off Sturgeon Bank. The sound speed profile from Fig. 3.1 was used, assuming as a first approximation no range dependence. Correction was made for seawater absorption loss (0.0012 dB/m at 12kHz), a surface reflection loss of 1 dB per bounce, and seabed forward reflection loss vs. grazing angle calculated using classic two-layer interface theory. Sediments in the Fraser River delta area are comprised of silty sands with assumed density and sound speed of 1900 kg/m^3 and 1600 m/s, respectively. Thus, seabed reflections have a 9.5 dB loss at normal incidence, decreasing with grazing angle and assumed to be 2 dB below the critical angle.

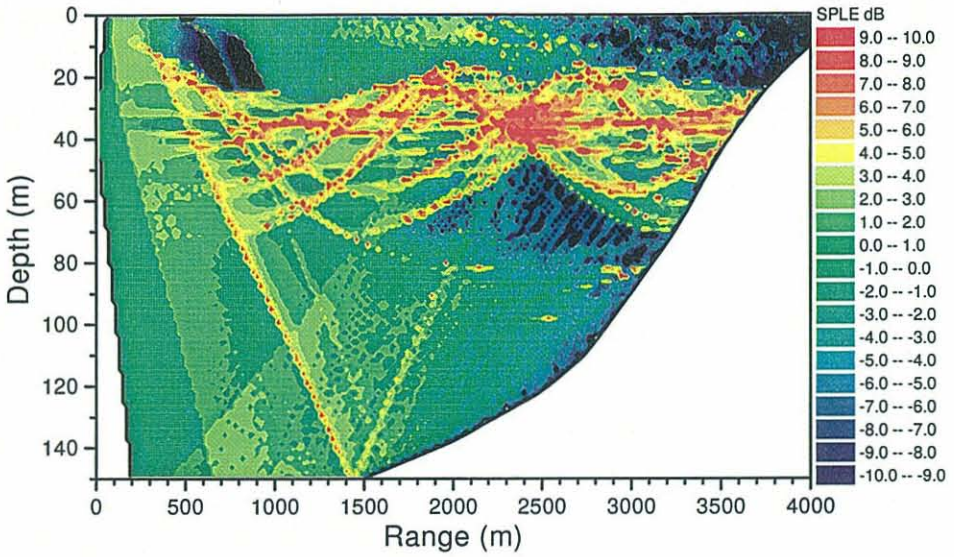

Figure 4.3: Cross-sectional distribution of modeled acoustic sound pressure level excess (dB), using bathymetry as shown and sound speed profile as in Fig. 3.1. Source located at 35 m depth.

Figure 4.3 shows the expected focusing of acoustic energy by boundary reflections and internal refraction. In this calculation the one-way sound pressure level has been referenced to a 20log[r] decrease, which removes the effects of spherical spreading leaving only the excess (denoted the sound pressure level excess, *SPLE*) variation due to propagation focusing. The figure shows the clear focusing of energy within the 20 to 60 deep sound channel, with *SPLE* values in excess of 10 dB. There is a particularly strong focusing region near 2500 m range and 40 m depth, with a defocusing (shadow) zone immediately beneath (50 to 80 m depth). There is a significant seabed interaction within the first 2000 m, creating to the observed higher levels of background clutter. The near-seabed *SPLE* decreases from 2000 to 3200 m range, then again increases dramatically near 3500 m range (the *acoustic shore*) where the sound channel intersects the seabed. These features can be seen in the data, and created the favorable detection conditions for fish schools shown for example in Fig. 4.1. Another important shadow zone is created in the near surface (<20 m depth) beyond 2500 m range. Fish located in this near-shore surface region would not be detectable, which is in accordance with the observations. During the surveys, Sockeye salmon were observed at the surface (and occasionally jumping) in this near-shore region.

5. 100 kHz Echo-Sounder Results:

The 100 kHz echo-sounder on the Vector provided a powerful imaging capability of the zooplankton and fish distributions beneath the ship. Figures 5.1 and 5.2 show two examples. In both images the seabed is clearly defined, and there is a strong scattering layer in the upper 5 m probably due to suspended sediments in the freshwater plume from the Fraser River. The background line near 80 m depth in both images is an artifact of the instrument TVG. Figure 5.1 shows a variety of fish and zooplankton aggregations,

especially near the seabed, that were typical features near the Fraser River mouth at Sandheads. The dense clouds between 60 and 80 m depth are likely zooplankton, and were a ubiquitous feature of these echo-sounder records in all areas of southern Strait of Georgia. Since no simultaneous net -samples of these zooplankton were taken, it is difficult to identify the exact species composition, although some reference to previous ecological survey results could be pursued. The more diffuse clouds of scatterers near the seabed, especially in the latter half of Fig. 5.1 are either larger zooplankton (such as Euphausiids) or herring. The intense vertical plumes extending upwards from the seabed are hypothesized to be composed of microbubbles created by decomposition processes within the newly deposited sediments at the river mouth. These plumes are commonly seen in the Sandheads area, but not further north or south. Figure 5.2 shows the rising freshwater plume from the Iona Island sewage treatment plant outfall, located roughly 4 miles seaward of Vancouver Airport. The intense aggregations of zooplankton are obvious. At this time the tide was ebbing and thus flowing southward, in the same direction as the Vector course. The southward-flowing plume remnants are seen at later times between 20 and 40 m depth. The intense acoustic scattering within the plume is likely due to high concentrations of suspended particles, with possibly some contribution from turbulent micro-structure scattering.

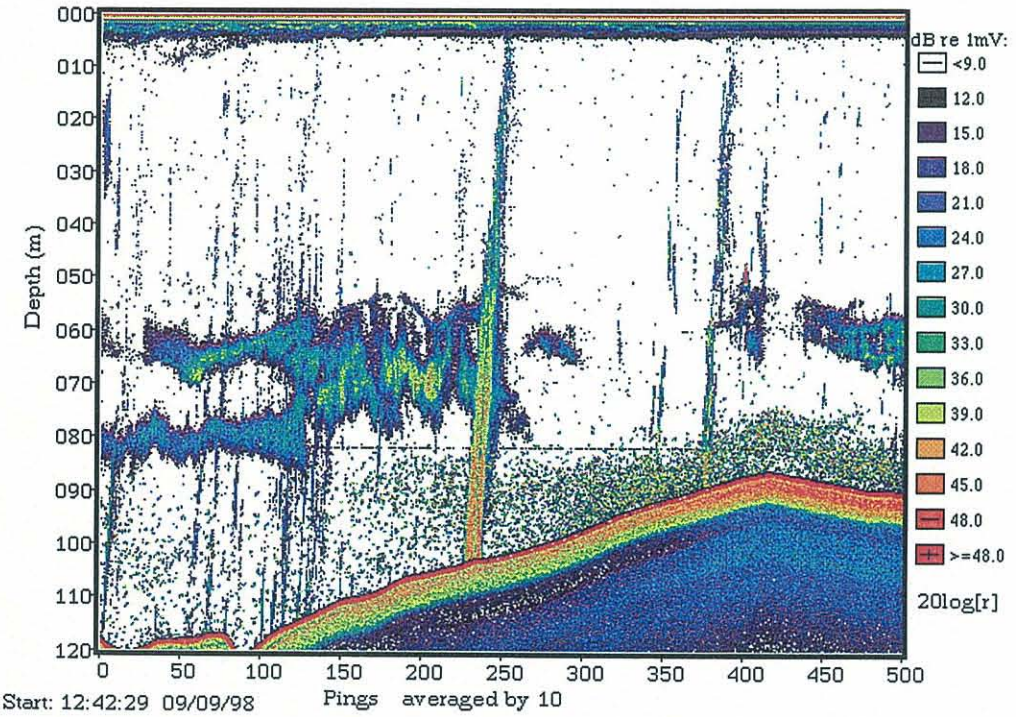

Figure 5.1: 100kHz echo-sounder raw intensity vs. depth and time image taken during a southbound transit near Sandheads starting 1242h Sept. 9th. Total duration is 16 min., 40 s.

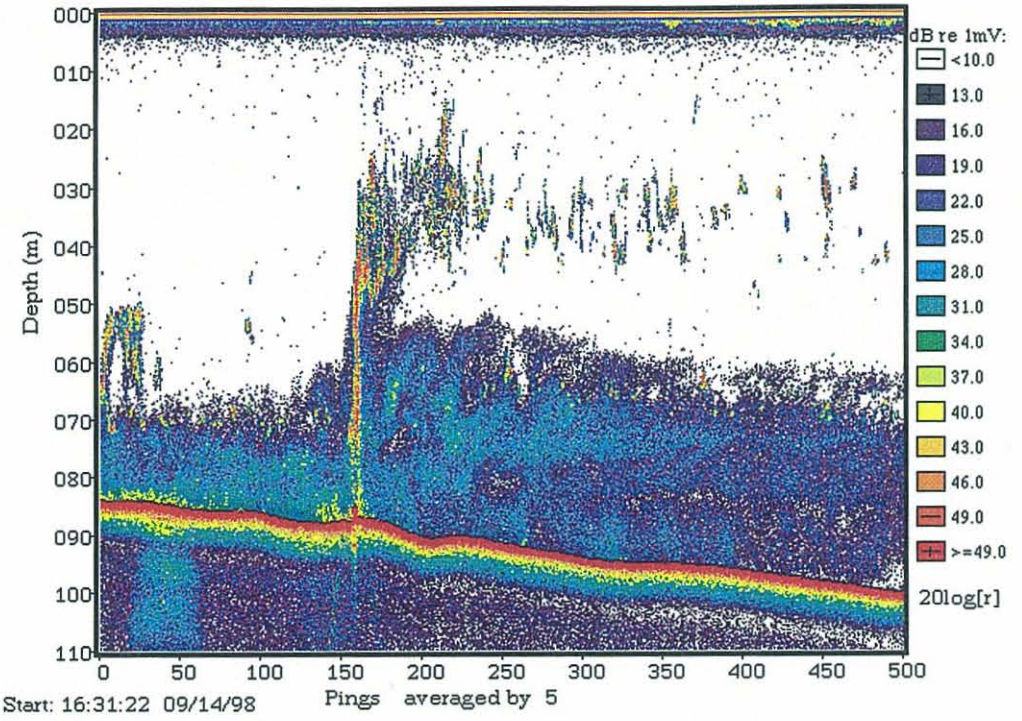

Figure 5.2: 100kHz echo-sounder raw intensity vs. depth and time image taken during a southbound transit over the Iona Island sewage treatment outfall at 1631h Sept. 14th. Total duration is 8 min., 20 s.

In the 100kHz echo-sounder data there is some evidence to support the hypothesized vessel-avoidance behaviour by the fish. Initial inspection of many hours of echo-sounder data uncovered no targets with $TS > -32$ dB in the upper 20 m, despite expectations that the majority of adult salmonids should be found near the surface. It seems reasonable to expect that salmon would avoid a vessel as large as the *Vector*, and the sampling volume of this narrow acoustic beam is very small immediately beneath the vessel. Assessment of this behaviour is complicated by the fact that with a single-beam echo-sounder the position of any particular fish target relative to the sounder beam cannot be known. A large fish on the edge of the beam would give the same echo strength as a small fish on the beam axis. This problem can be circumvented in an ensemble averaged sense by examining the echo amplitude statistics, specifically through calculating echo amplitude probability density functions (PDFs), as described in Clay (1983) and MacLennan (1990). In this formulation the echo-amplitude (e = √backscatter cross-section in m^2) PDF, $w_E(e)$, can be given by a convolution integral of a Rayleigh PDF for single fish scattering and the PDF arising from beam-pattern effects, i.e. as

$$w_E(e) = \int_0^1 \frac{w_T(b) \cdot w_R(e/b)}{b} db ,$$

where $w_T(b)$ is the PDF for observing an amplitude b for scatterers randomly distributed in the transducer beam. Ehrenberg et al. (1984) determined an empirical relation for $w_T(b)$ for cylindrical transducers of radius a_t of the form

$$w_T(b) = \frac{a_1}{(k \cdot a_t)^2 (b + a_2)^{a_3}}$$

where k is the acoustic wavenumber, $a_1 = 2.03$, $a_2 = 0.01$, and $a_3 = 0.83$, for $b > 0.005$.

The Rayleigh PDF for fish echo amplitudes is given by

$$w_R(e) = \frac{2e}{\sigma} \exp\left(-\frac{e^2}{\sigma}\right)$$

where σ is the mean backscatter cross-section (m^2) of the fish targets, in this case taken in ventral-incidence. All these PDFs are normalized so that the integral over all amplitudes is unity. These equations enable prediction of the expected PDFs for the various fish species (i.e. adult salmon and herring) expected in the area and observed with the *W.E. Ricker* trawls. Then, these predictions can be compared to echo amplitude PDFs extracted from the echo-sounder data over several depth intervals, as shown in Figure 5.3. In this mixed species environment the data PDFs show several distinct regimes, which can be roughly divided into three groups: small (e < 0.007 m or FTS < -43 dB), medium (0.008 m < e < 0.03 m or -42 dB < FTS < -30 dB), and large (e > 0.04 m or FTS > -28 dB) sized fish targets. These three groups can be loosely associated with herring, juvenile salmon, and adult salmon, respectively. Fig. 5.3 clearly shows that the data PDFs from nearer the surface contain significantly lower numbers of the medium and large size groups. Predicted echo-amplitude PDFs closely match the data in the medium size range, with the data bounded by curves with mean Rayleigh cross-section of 1.8 to 4.5 x 10^{-4} m^2 (TS increasing from -37 to -33 dB) with increasing depth. The blue curve in Fig. 5.3 shows the expectation for small numbers of adult salmonids (TS = -23 dB), which loosely agrees with the data from the 32 - 40 m depth interval. However, in the first two depth intervals the probability density for the larger targets is negligible. This echo-sounder evidence suggests that larger fish are either naturally found at greater depths or actively avoiding the region roughly 20 m below the ship.

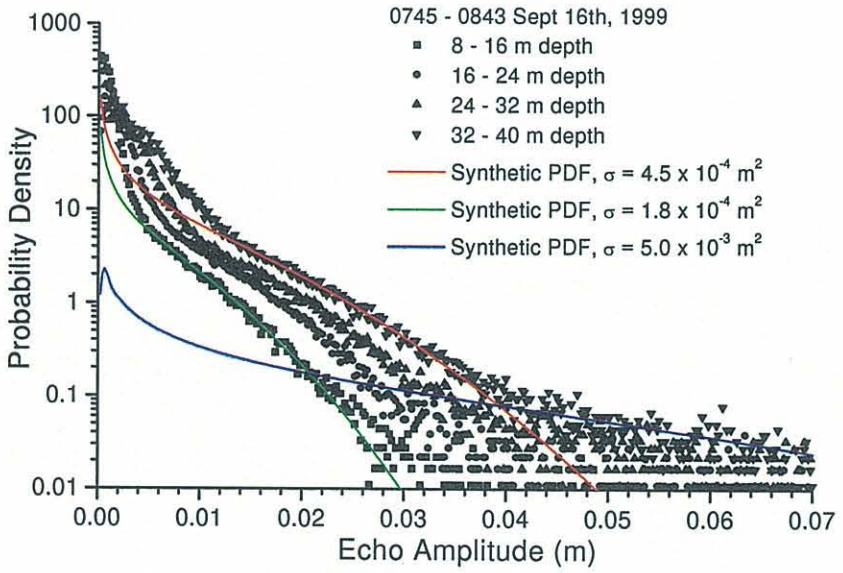

Figure 5.3: Comparison of experimentally derived and reference Probability Density Functions of echo-amplitude taken with the 100 kHz echo-sounder on the survey ship *Vector*. The data spans 12000 transmissions between 0745 and 0843 Oct. 16th, 1999.

6. Mobile Split-beam Echo-Sounder Surveys:

Comparison surveys with the EK-500 120kHz split-beam echo-sounder were conducted with the *Grebe* on Sept. 9th through 12th. These surveys were conducted at the same time and in the same location as on-shore looking IRFS surveys, with a typical example of survey tracks shown in Figure 4.2. A typical example echogram from one of these cross-shore tracks in a region just north of Sandheads is shown in Figure 6.1. In the echogram the detected seabed is clearly visible as the black line overlying the red seabed scattering region. Several distinct schools of (likely) herring with volume scattering strength > -40 dB (re 1 m^{-1}) can be seen near the seabed in 40 to 80 m water depth. These herring schools are not of uniform density but rather have a coarse, granular nature. Also, a few smaller schools (herring balls) can be seen near the surface. In the latter part of the transect a more diffuse cloud of zooplankton extends outwards from the seabed at depths of 80 to 100 m. All these features are similar to fish schools and zooplankton clouds seen with the 100kHz echo-sounder on the *Vector*.

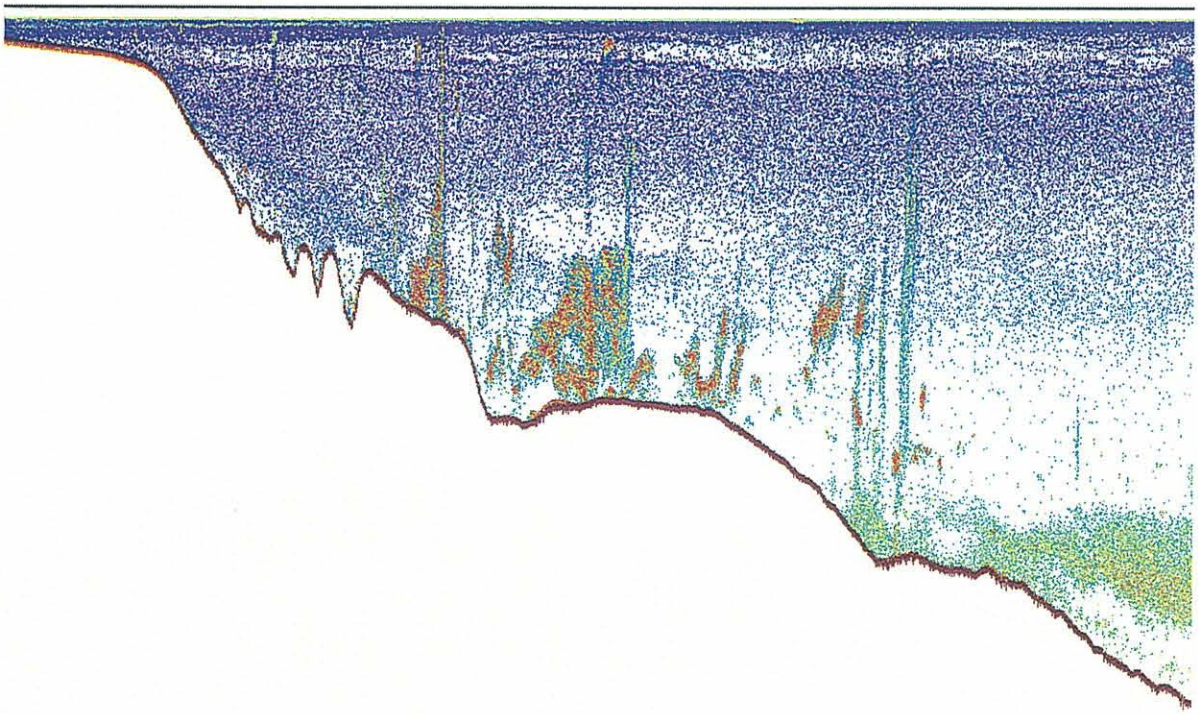

Figure 6.1: Calibrated volume scatter strength vs. depth and time echo-gram from the 120 kHz EK-500 echo-sounder on the Grebe. Data taken from a cross-shore track north of Sandheads at 1408h - 1429h, Sept. 11th. Depths from 4.8 m to 112.3 m. Volume scatter strength from -80 (blue) to -40 (red) dB re m^{-1}.

A great advantage of this split-beam echo-sounder is its ability to extract the fish target position within the transducer beam so that corrections for beam-pattern can be made. The EK-500 can be set to automatically search for single targets (i.e. with echo duration ≈ pulse length), make the beam-pattern correction, and store in a separate data file. Figure 6.2 shows example histograms of depth and dorsal target strength from data taken during several transects north of Sandheads on Sept. 11th (i.e. including data shown in Fig. 6.1). The depth distribution shows a broad peak between 30 and 70 m, but this has not been corrected for the fact that because of the sloping bottom not all depths were equally

sampled. Also, there is the possibility that the single target detector has mistakenly extracted scattering data from within the herring schools lying near the seabed in 40 to 80 m of water (e.g. as in Fig. 6.1). The dorsal TS distribution shows a peak at the lowest values near -60 dB (re 1 m^2), presumably due to zooplankton, with sub-peaks near -52 dB, -45 dB, and -38 dB. These three dorsal TS values correspond to expectations for juvenile herring, adult herring, and juvenile salmon, respectively. In terms of target strength, a threshold value of -32 dB should distinguish adult salmon from other fish. In this data, only 85 targets or 6.3% of the total have TS values > -32 dB, with most of these occurring at depths between 40 and 70 m. Only one -30 dB target (i.e. a Sockeye) was observed in the upper 20 m. This lack of salmon targets is probably due to some combination of low abundances in the survey region and boat avoidance behaviour. Again, there is potential for inclusion of non-point targets through the target detector which may be contaminating this data.

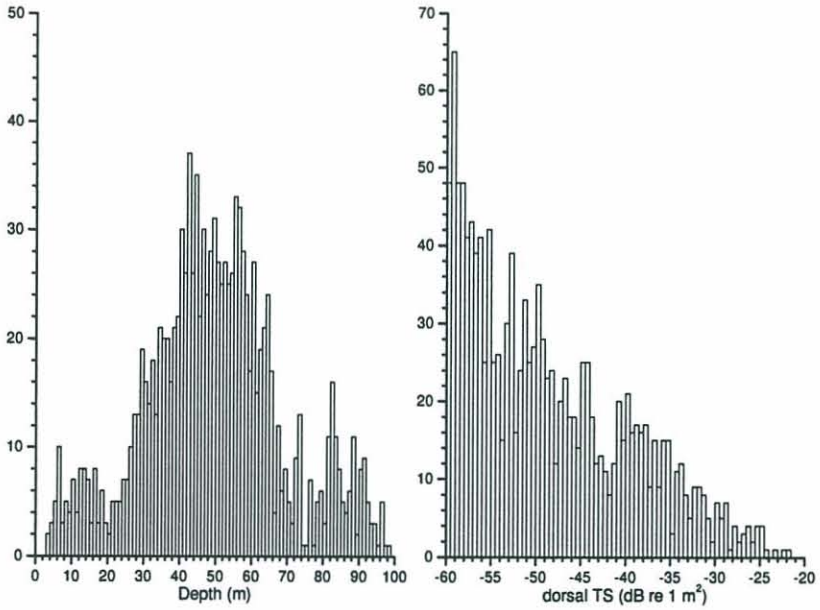

Figure 6.2: Histograms of single target depth and dorsal TS taken with 120kHz EK-500 split-beam echo-sounder on the Grebe, from several cross-shelf transects at 1402h - 1451h, Sept. 11th north of Sandheads. Total number of targets = 1343.

7. Towed 330kHz Sidescan Results:

Evaluation surveys with the 330 kHz towed sidescan were only conducted on Sept. 15th and 16th, with the conventional sidescan mode used on Sept. 15th and the vertical sector scanning mode on tested on Sept. 16th. In spite of the early migration of the Sockeye salmon into the Fraser River, sufficient numbers of fish targets were observed in the near-surface waters to allow a reasonable assessment of this technology. A detailed evaluation of this data can be found in a manuscript currently under review with *Fisheries Research* (Trevorrow 2000). This section will present a brief overview.

Perhaps the most important parameter in understanding the performance and limitations of a sonar system is the background noise level. In general this will be a combination of systemic noise and environmental reverberation. In this specific application, the two most important noise sources are backscattered reverberation from the sea surface and electronic noise. Figure 7.1 shows typical background noise curves for the two deployment modes, converted to apparent *TS* using the system calibrations and the standard sonar equation. Each of these curves was averaged over roughly 12,000 individual transmissions, with surface-contaminated portions of the vertical sector scans removed. During these tests the system gain was set near maximum in an attempt to detect smaller fish and to properly resolve the background noise levels. Apart from a small direct surface echo, the vertical sector scan noise curve shows a rather smooth variation similar to the A/D threshold, indicating that its source is likely electronic noise in the cable and waveform detection circuit (i.e. generated after the TVG amplifier). After the first surface return near 18 m range, the sidescan mode exhibited a 2 to 10 dB higher noise level due to surface backscattering through the transducer side-lobes.

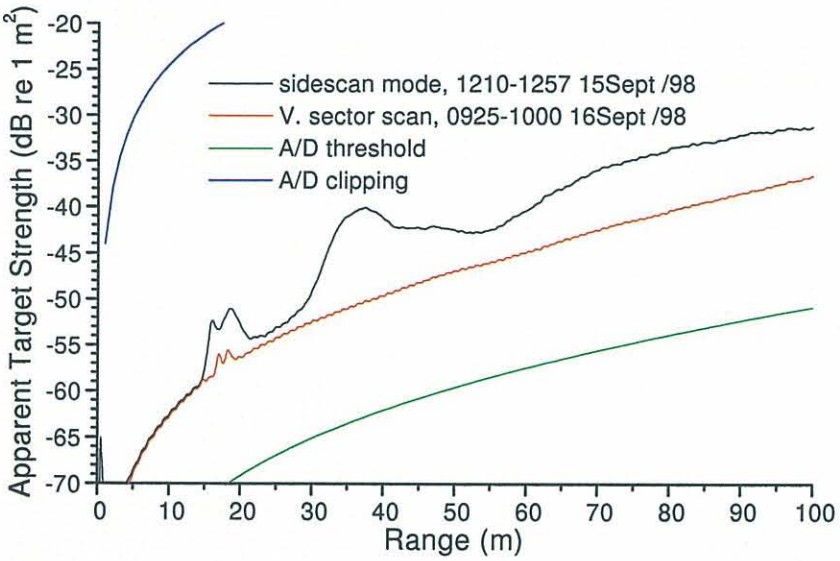

Figure 7.1: Comparison of time-averaged background reverberation level vs. range for the sidescan and vertical sector scan modes of the 330kHz sonar. Curves corresponding to the A/D converter threshold and clipping values are shown for reference.

Software was written to display, identify, and quantify fish echoes from the sidescan and vertical sector scan data. In general, the fish targets appeared as isolated, short duration (1 to 3 range sample) peaks with apparent *TS* up to 27 dB in excess of the noise levels. For target recognition purposes two main criteria were applied: i) the apparent *TS* maxima at a given range had to exceed a detection threshold given as the noise curve plus 9.0 dB, and ii) the target width had to be ≤ 4 range samples (20 cm). The +9.0 dB detection threshold was found by trial and error to most effectively separate the fish targets and background noise. In the vertical sector scan mode targets also had to be more than 1 m away from any surface clutter. In both geometries it was possible for multiple hits on the same target. To resolve this the maximum apparent *TS* for a particular target was used. For the sidescan mode this corresponded to the point of closest approach as the target

passed through the beam. For the vertical sector scan mode the maximum apparent *TS* was chosen among targets falling within a small range-depth-time window. With the higher noise levels in the sidescan mode the detection threshold was sufficiently high that only a few unambiguous fish targets were observed within the first 30 m. This limitation in combination with the inability to resolve the target depth rendered this sidescan mode ineffective for surveys of this type. Henceforth only the vertical sector scan results will be discussed.

During the five tows on Sept. 16th in the vertical sector scan mode a total of 563 individual fish targets were detected. Figures 7.2 and 7.3 summarize the raw *TS*, range, and depth distributions of these targets. These apparent *TS* values have yet to be corrected for biases induced by acoustic refraction and transducer beam-pattern (i.e. these are biased estimates of the true fish *TS*, denoted *FTS*). Clearly, the relatively high detection threshold limits the detection of successively larger fish with increasing range, such that herring would not be detectable beyond 42 m range, and only a modest fraction of the adult salmonids would be detected near 100 m range. Note the absence of fish within the first 20 m, which is due to a combination of the smaller sampling volume at close range and possibly boat avoidance behaviour. Clearly, the sampling volume at close range, particularly in the near-surface and at greater depths, is limited by the vertical scan aperture (30°). At all ranges the maximum apparent *TS* values were near -22 dB, which is in agreement with our expectations for adult salmonids. The apparent decrease in fish density with range in Fig. 7.3 is due to the increasing detection threshold removing the smaller targets. Overall, in this raw data there appears to be a slightly higher density of fish targets in the upper 20 m.

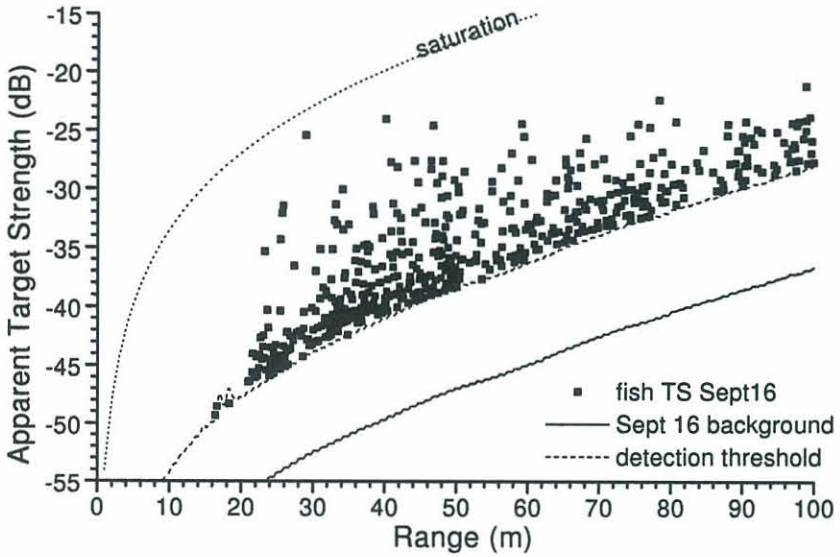

Figure 7.2: Summary of apparent fish target strength vs. range for 330 kHz vertical sector scan trials on Sept. 16th. A total of 563 targets were detected over a total towing distance of 12.6 km.

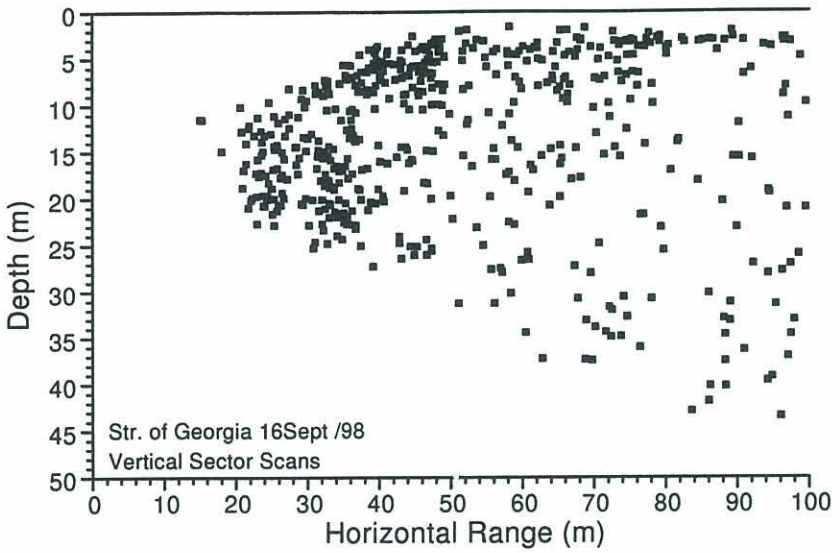

Figure 7.3: Raw, uncorrected horizontal range vs. depth distribution of detected fish targets from 330 kHz vertical sector scan trials on Sept. 16th.

The apparent fish depth and *TS* need to be corrected for acoustic refraction effects induced by the strong temperature and salinity gradients near the surface. A ray-tracing code due to Bowlin et al. (1992) was used to calculate ray trajectories and incident sound pressure levels given the sonar depth, fish target location, and the sound speed vs. depth profile. Eigenrays connecting the source and a horizontal range vs. depth matrix of possible fish locations were computed for a launch angle interval of ±15° from horizontal. This near-surface refractive environment induces two kinds of bias in fish detection. Firstly, a bias in the apparent target depth arises from the difference between refracted and straight-line paths, such that (under these conditions) the apparent target depth is always less than the true depth. This bias increases with horizontal distance and is larger near the surface. A maximum depth bias of 3.2 m occurs within the top 5 m at 100 m range. The second type of bias is a propagation focusing effect that modifies the apparent fish *TS*. This acoustic propagation focusing effect is not included in the spherical spreading model implicit in the standard sonar equation. This *TS* enhancement exhibits a more complicated spatial distribution, generally increasing with distance, such that by 100 m range the bias spans the interval -2.4 dB to +3.0 dB (relative to spherical spreading). Using the ray-tracing results, corrections for both types of refraction-induced bias can be applied to each individual fish target.

Finally, there are two further sonar performance corrections that must be applied to the overall results: namely for target detectability and transducer beam-pattern bias (*BPB*). Detectability can be defined as the ratio of detected to true number of targets passing through the vertical sector. It is a complicated function of true *FTS*, target range and depth, and sonar operating parameters such as noise threshold and transducer beam-pattern. When the fish targets are detected away from the transducer principal axes the apparent *TS* will be reduced. However, for this single-beam sonar at a given ping it is impossible to know the exact location (with respect to the transducer axes) of an

individual fish target. Thus, only averaged *BPB* corrections can be applied. These two sonar performance parameters are intimately related.

To quantify performance estimates a numerical simulation of the sonar operation was devised. The method evaluates the average detectability and *TS* bias over a large number of trials with fish targets of known *FTS*, depth, and horizontal distance as they are advected past the vertically scanning sonar beam. The sonar depth, ping rate, and vertical scanning parameters were the same as actually used. For each detection trial, a fish target was advanced along a path perpendicular to the vertical sector at the nominal towing speed (2 $m \cdot s^{-1}$) from -100 m to +100 m relative to crossing-point of the main beam axis. For each trial the phase of the sonar vertical scan was randomized. For each synthetic ping in a trial the target position angles and beam deviation loss were computed, and the apparent fish *TS* then compared with the measured detection threshold (the noise level vs. range from Fig. 7.1 + 9.0 dB). As done with the real survey data, the maximum apparent *TS* among several target hits during each trial was selected. This simulation was performed over a matrix of horizontal distance (2 m increments to 100 m) and depth (1 m increments to 50 m) target positions, with results averaged over 5000 trials at each location.

As expected, the sonar was unable to detect targets outside the 30° vertical scanning sector, and the fish detectability and *TS* bias were nominally uniform with angle within this sector. Thus, the analysis can proceed using results averaged over this 30° vertical sector. Both the detectability and *BPB* results are strongly influenced by the detection threshold relative to the *FTS*. With increasing horizontal range the target detectability decreases due to the need for the fish target to be detected closer to the transducer principal axes (where the *BDL* is less) in order to exceed the detection threshold. This effect is more pronounced with smaller targets, such that (for example) with herring of $FTS < -40$ dB the detectability is less than roughly 50% at all ranges. For fish with $FTS \leq -30$ dB there exists a range where the detection threshold exceeds the *FTS*, forcing the detectability to zero. At close range the detectability drops as some of the fish slip past the smaller sonar sampling volume. The detectability increases again at ranges < 5 m as the fish become detectable through the transducer side-lobes. For a given *FTS*, the bias in apparent *TS* decreases with increasing horizontal distance as the fish detection threshold selects only those targets closer to the transducer principal axes (i.e. with smaller *BDL*). Similarly, at a given horizontal range fish with smaller *FTS* exhibit a smaller *TS* bias.

Corrections for target *BPB* and detectability can now be applied to the sonar data. The application of these average corrections proceeds under the assumption that each observed fish target is a biased sample of the overall range-depth-*FTS* population within this 30° vertical sector. Firstly, for each fish target the average transducer *BPB* can be interpolated from within the simulation results. This is an iterative process, as the amount of *BPB* that produced the apparent *TS* is dependent on the unbiased *FTS*, however the iterations quickly converge to a unique result. Larger targets at closer range are compensated more strongly, with an overall average *TS* correction of +1.1 dB. It must be understood that these averaged *BPB* corrections cannot recover the true *FTS* for each target, thus the corrected results should only be used in an averaged sense. Next, for each *BPB*-corrected target the detectability coefficient is interpolated from within the

simulation results. The average detectability for this data is 58%. Finally, dividing each fish sample by the detectability produces an estimate of the true fish population density vs. range, depth , and *FTS*.

Including the detectability corrections, the estimated true number of fish targets (of all species) was 867 over the total survey track length of 12.62 km. The total sample volume can be computed by multiplying the track-length by the planar area of the vertical sector (2460 m^2) scanned by the sonar. This produces a total sampled volume of 31 x 10^6 m^3, for an overall fish density (all species) of 28 x 10^{-6} per m^3. Assuming that some fraction of these fish are adult salmon, this estimate is in reasonable agreement with several other studies on adult salmonids. Somewhat lower densities (1 to 2 x 10^{-6} per m^3) of sockeye salmon were observed during conventional echo-sounder surveys conducted in this same area by Levy et al. (1991), however that study was found to under-estimate the true salmon abundance by roughly 50% (based on comparisons with run re-constructions). A side-looking sonar survey of adult salmonids in Cook Inlet, Alaska (Tarbox & Thorne 1996) produced densities of 0.5 to 19 x 10^{-6} per m^3, again with a detectability of roughly 50% (based on comparison with commercial and test fishery results). In this region we can produce a crude estimate of the salmon density by dividing the daily salmon escapement into the Fraser River for Sept. 17th (45,200 from Fig. 2.2) by the area of a semi-circle with radius equal to a salmon daily migration distance (roughly 12 km, Quinn and terHart 1987) and assuming a depth extent of 30 m. This crude estimate is 6.7 x 10^{-6} per m^3, which is entirely consistent with our estimates.

To examine the range, depth, and *TS* distributions these corrected results now have to be appropriately averaged, with results shown in Figure 7.4. The *TS* distribution was derived by selectively averaging in horizontal range the detectability-corrected *TS* distributions computed within 2 m horizontal range bins. Averages for a particular *TS* bin were only computed over a range interval where the detectability was >0.1. In Fig. 7.4a the corrected *TS* distribution spans the interval -46 to -22 dB, with peak at -41 dB. Within this distribution 10.0% of the fish have $TS \geq -30$ dB, which is a threshold that clearly distinguishes adult salmonids. Using the expected *FTS* distribution for adult salmonids, we can conclude that approximately 24% of the overall fish targets were adult salmonids (lumping chinook, chum, and sockeye together), corresponding to a volumetric density of 6.7 x 10^{-6} per m^3. The remaining 76% will be dominantly juvenile salmon. This ratio of adults to juveniles is in agreement with the trawl results (17% vs. 83%).

The depth distribution (Fig. 7.4b) is compensated for the fact that only depths falling within the 30° vertical scanning sector are sampled. For example, at the sonar depth (18 m) the entire 100 m range is covered, while in the top 2 m only 38% of the total range is insonified. The depth distribution shows clearly a strong preference for the top 22 m (82% of the total), with a peak between 4 and 6 m. This is in direct agreement with ultrasonic tagging studies conducted on sockeye salmon by Quinn & terHart (1987), and confirms the earlier assumption that chinook, chum, and juveniles exhibit similar depth preferences to sockeye.

Finally, the horizontal range distribution must be compensated for the increasing volume of the 30° vertical sector with range, the non-uniform depth-distribution, and the

increasing detection threshold with range. The corrected range distribution (Fig. 7.4c) shows that very few fish were detected within the first 20 m of the sonar, with a significant excess (61% of total) between 20 and 48 m. The most likely explanation for this is that fish have moved horizontally out of the zone extending 20 m laterally from the port-side of the vessel (where the sonar was towed). If there was no vessel-avoidance behaviour this distribution should be uniform in range. A similar vessel-avoidance reaction was observed for schooling epi-pelagic fish with a multi-beam sonar by Soria et al. (1996).

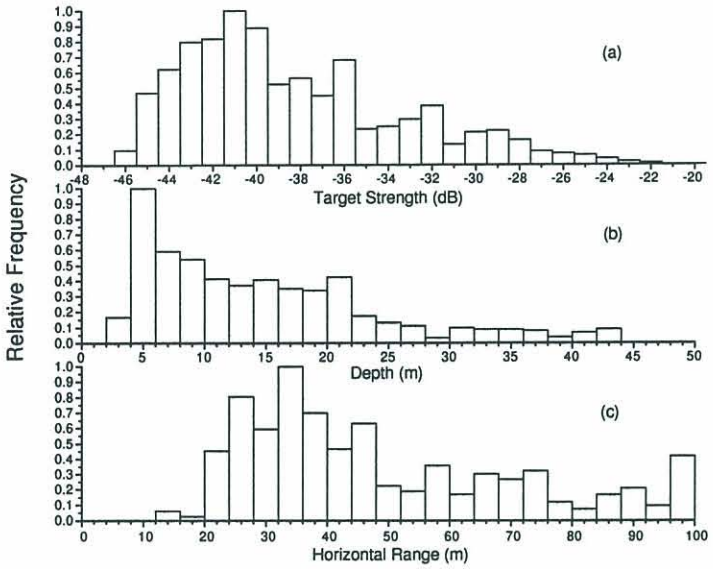

Figure 7.4: Distributions of fish target strength, depth, and horizontal range compensated for refraction effects, beam-pattern bias, and target detectability from the 330 kHz vertical sector scan trials.

8. Moored Inverted Echo-Sounder Results:

The moored inverted echo-sounder WASP was deployed and operated successfully from 1805h Sept. 8th until 1424h Sept. 16th, 1998 at a location roughly 2 miles North of Sandheads. The intention was to evaluate the feasibility of a moored echo-sounder for monitoring near-surface fish and zooplankton populations, and possibly extract fish occurrence vs. depth distributions, which are an important parameter in understanding fish detectability with the IRFS. The most basic data product from WASP was the instantaneous range to the surface, which contains variations due to both tides and surface waves. Figure 8.1 shows the 30-second averaged surface height for the entire deployment. This is clearly dominated by tides and is entirely consistent with official tidal predictions for Sandheads. This clearly defined surface can be used as reference for all further analysis. Additionally, during periods with winds sufficient to cause white-capping, WASP provided a measure of bubble plume penetration. In this data set significant bubble penetrations only occurred on the nights of Sept. 11/12th and Sept. 14/15th, with maximum penetrations of up to 3.4 m.

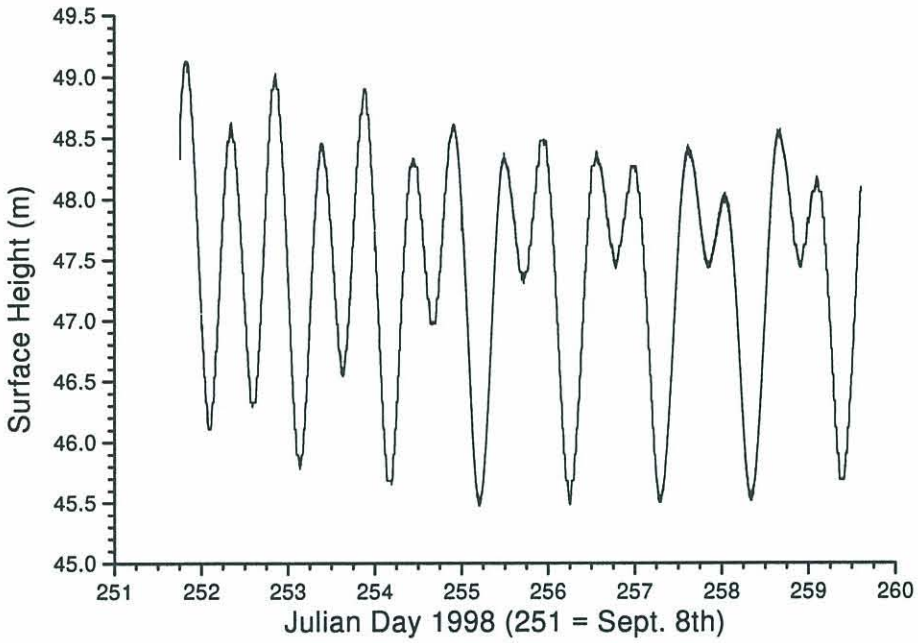

Figure 8.1: 30-second averaged surface height variations from WASP.

The WASP captured many events of herring school and zooplankton nocturnal migration. Figure 8.2 shows fish school (or parts thereof) activity near mid-day. Occasional near-surface (< 10 m) schools or balls advected through the WASP sonar beam were observed nearly every day. Also, deeper schools near the lower range of WASP sampling were commonly observed (the 32 m lower sampling limit is still 15 m above the WASP instrument). The vertical extent of these schools below 32 m is impossible to assess from this data. These schools are presumed to be herring, from reference to the net trawls performed in this area by the *CCGS W.E. Ricker* on Sept. 16th. Schooling behaviour during daylight hours is commonly observed in herring, and is further consistent with the EK-500 echo-sounder survey results described earlier. It is conceivable that the fish could have locally congregated around the WASP instrument and mooring, generating a possible source of bias in such measurements. Figure 8.3 shows an example of the daily zooplankton downwards migration just before dawn on Sept. 12th. In the evening hours (the upwards migration is not so distinct) zooplankton congregate in a layer between 8 to 16 m depth. This layer was observed to migrate downwards, presumably to the seabed, with a speed of roughly 1 cm/s. No zooplankton sampling was performed, so the identity of these animals in unknown. If the identity and size of these animals could be established from previous ecological studies of the area, then the WASP calibrations could be used to assess zooplankton population densities.

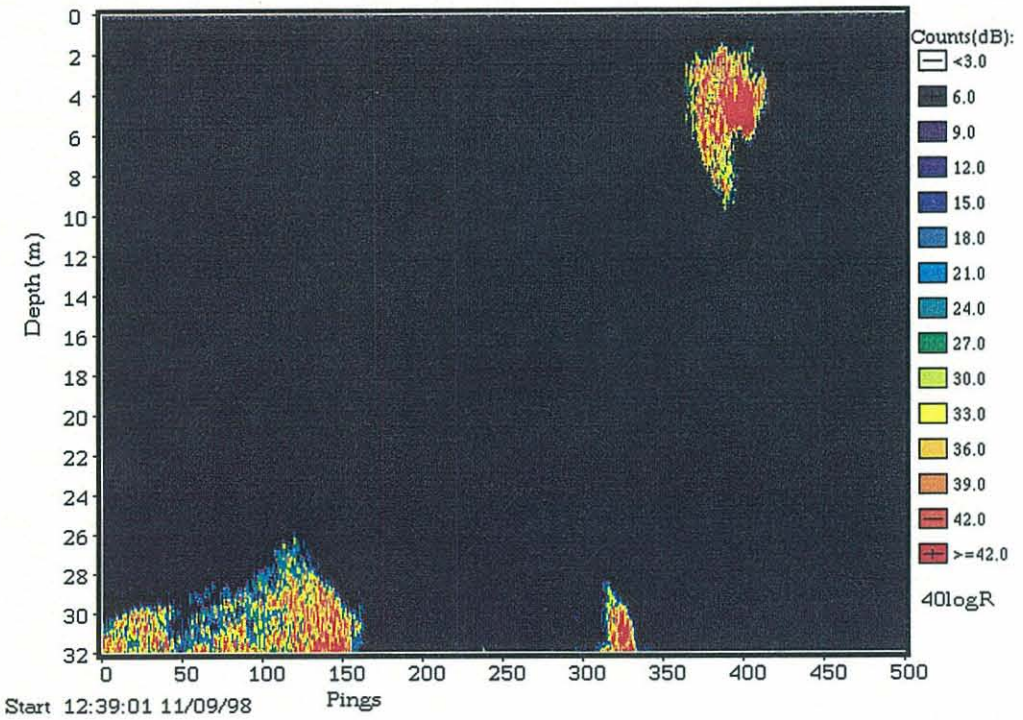

Figure 8.2: WASP raw intensity vs. range and time (8 min., 20 s total duration) at 12:39h on Sept. 11th.

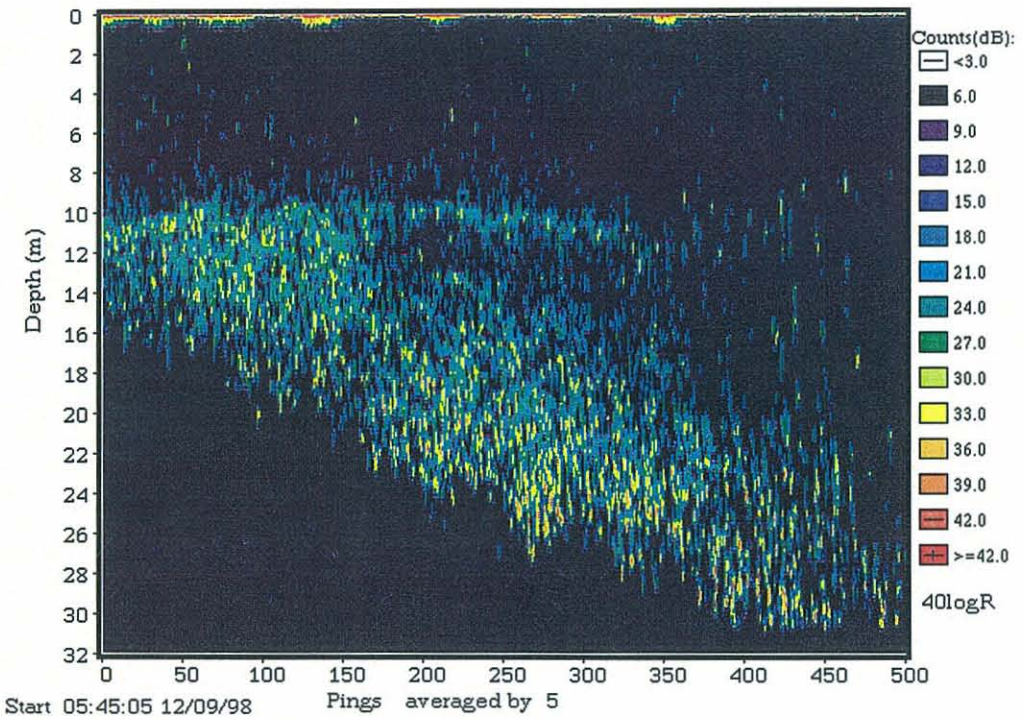

Figure 8.3: WASP raw intensity vs. range and time (41 min., 40 s total) starting at 0545h Sept. 12th.

Single targets within the WASP data can be analyzed statistically in a similar way to those observed with the 100kHz echo-sounder on the *CCGS Vector*. Similar single-target selection criteria were used, i.e. using a 2 ping average from the surface to 30 m depth,

targets were selected with pseudo-TS > -50dB, range dimension ≤ pulse length, and duration < 4 s. Special routines to reject targets within fish schools and surface bubble plumes were implemented. Also, in order to better isolate individual herring from their schools and to assess zooplankton populations, it was useful to focus any statistical analysis on night-time periods (i.e. from 2000h to 0500h). Similarly to the 100kHz echo-sounder on the *Vector*, we use an echo amplitude taken as the square-root of the calibrated back-scatter cross-section (in m^2). A comparison of the measured echo-amplitude probability densities with reference curves for herring and salmon from the 7 nights during the WASP deployment is shown in Figure 8.4. As with the 100kHz sounder, there is strong agreement in between the data and synthetic PDF for herring over the echo amplitude range 0.003 to 0.014 m, corresponding to a pseudo target strength interval of -50 to -37 dB (re 1 m^2). The synthetic PDF for herring is based on a mean cross-section of 5 x 10^{-5} m^2, or -43 dB re 1 m^2. There is a clear change in scattering regime at echo amplitudes above 0.014 m (-37 dB), and presumably this value could be used as a threshold to separate herring from salmon. However, the comparison between data and synthetic PDF for adult salmon is not as good, presumably due to insufficient numbers of these larger targets observed with WASP. The fact that the synthetic PDF amplitude for salmon had to be reduced by a factor of 20 suggests that the numerical abundance of salmon was only 5% that of herring. Since it is less likely that salmonids would actively avoid a quiet, moored instrument such as WASP, it can be concluded that very few salmon were available for observation with this instrument. This is in accordance with acoustic results from the IRFS, 100kHz and 120kHz echo-sounders, and the IMX sidescan.

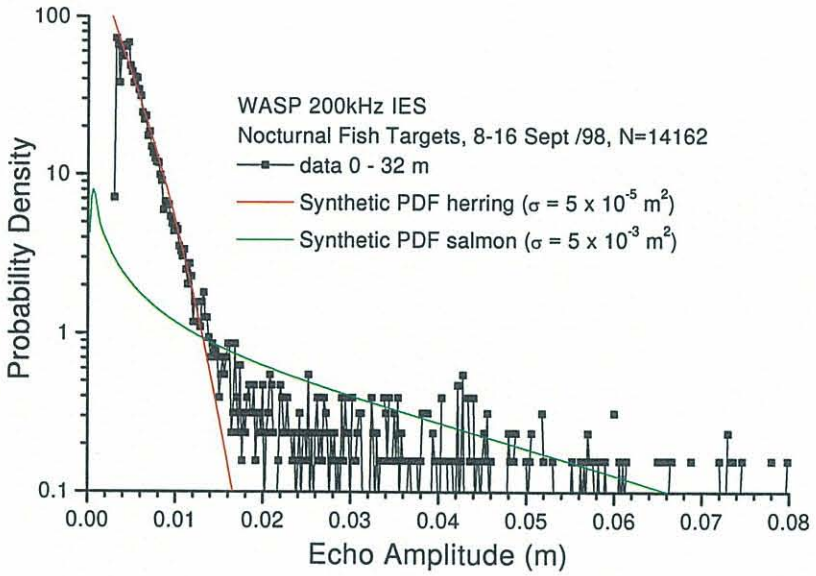

Figure 8.4: WASP single-target echo-amplitude probability density from night-time data (2000h to 0500h) Sept. 8th through 16th. Reference curves correspond to expected Rayleigh distributions for herring and salmon. Salmon synthetic PDF divided by 20.

9. Discussions and Recommendations for Further Work:

These results taken all together present a complicated picture of the horizontal distributions of fish and zooplankton populations in the survey area, with many unanswered questions remaining. Clearly, this was a complicated working environment, both in terms of the physical oceanography of the Fraser River plume region and the multi-species fish and zooplankton populations. Although the original intent of using the various high-frequency echo-sounders was to provide ground-truth salmonid data for the 12kHz IRFS, these other instruments also produced intriguing and challenging data on zooplankton and herring populations.

In contrast to the August 1997 surveys with the IRFS, very few adult sockeye were observed with the IRFS in these Sept. 1998 trials. The most likely explanation for this is that the sockeye had already moved into the near-surface and shallows of Sturgeon and Roberts Banks by the time these acoustic surveys began on Sept. 9th. Large numbers of Sockeye were visually observed at the surface and jumping out of the water in the near-shore areas near Sandheads and in the lower Fraser River on Sept. 9th through 14th. This was confirmed by riverine escapement data from the PSC, which indicated that these Adams River sockeye began migration roughly 10 days earlier than historical expectations. Net trawls performed by the *W.E. Ricker* on Sept. 16th uncovered only 1 adult sockeye and only 6 other adult salmon over roughly 26 km of trawl effort. Also, single- and split-beam echo-sounders on the *Vector*, *Grebe*, and the moored WASP uncovered only weak evidence for small numbers of adult salmon in the offshore waters. Moreover, acoustic propagation results for the IRFS operated in an on-shore looking mode indicated that a near-surface (upper 20 m) shadow region existed at ranges >2000 m, likely obscuring any fish targets present in the near-shore areas near Sandheads.

All of the echo-sounders and the IRFS produced evidence for herring schools aggregated near the seabed in 60 to 100 m of water on the slopes of Sturgeon Bank, to the north of Sandheads. These schools were observed to have vertical dimensions from 3 to 30 m, and horizontal dimensions (from the IRFS) of 10 to 100 m. The identity of these fish was established from the *W.E. Ricker* trawl results, which uncovered copious quantities of herring in this region. Furthermore, from examination of echo-amplitude statistics from the moored and vessel-based echo-sounders, scattering statistics consistent with herring-sized fish were observed. Occasionally, smaller herring balls were observed close to the surface with WASP and EK-500 echo-sounders. Although our initial survey attempts were unsophisticated, through combining the large areal coverage provided by the IRFS with the high-resolution vertical echo-sounding and the species identity provided by net trawls, it was possible to produce a more complete picture of the herring distribution.

Some evidence for vessel-avoidance behaviour by the fish (both herring and salmon) was uncovered in the IMX sidescan, EK-500 echo-sounder, and 100kHz *Vector* echo-sounder data. The corrected horizontal distribution data from the IMX sidescan, which showed a distinct lack of targets within a 20 m zone near the Vector, was the most convincing. Similarly, the 100 kHz echo-sounder on the *Vector* showed no large fish targets within the upper 20 m and statistical evidence for increasingly larger herring-sized fish at greater depths. Although the vessel avoidance behaviour should have been much less

pronounced for the EK-500 surveys on the *Grebe*, a similar lack of larger (salmon) fish targets in the upper 20 m was observed, in spite of the fact that the Grebe surveys probed much closer to the edge of Roberts and Sturgeon Banks. These problems pose a significant limitation in the use of echo-sounders for the assessment of the vertical distribution of salmon targets, which is a crucial component for quantitative assessment using the IRFS. A conclusion from this is that the vertical sector-scanning approach with the IMX sidescan is the most practical for assessing the vertical salmon distributions.

In general, the results discussed in this report present a number of challenges for further development of this system. Both the Aug. 1997 and Sept. 1998 studies have shown the importance of understanding boundary reverberation and acoustic propagation effects. Work on acoustic modeling of these effects has been initiated, and these two data sets provide excellent test data to compare and refine the modeling efforts. Finally, given the experience provided by these two IRFS field trials, it seems practical to focus further field trials with the IRFS on regions with practical fisheries management applications. Specifically, this implies targeting salmon migration either through Johnstone Strait or the Strait of Juan de Fuca. Some consideration by the authors of the feasibility of salmon monitoring stations in Johnstone Strait is contained in a separate proposal. It is also feasible to use the IRFS for study of spawning herring schools in shallow waters in areas such as Baynes Sound or Barclay Sound.

The instrumentation discussed herein could be improved in various ways.

1. A second, higher frequency side-looking sonar could be added to the IRFS towfish. This second sonar would operate at a higher transmission rate suitable for sampling the inner 500 m of the survey area. This range could be adequately covered by a sonar operating near 50 kHz. It would probably be sufficient to use gated cw pulses, thus simplifying the data acquisition systems but requiring more signal lines in the tow-cable.
2. Implementation of a multi-channel coherent receiver, converting the IRFS into a phased array. This would enable simultaneous monitoring over a horizontal sector rather than a narrow horizontal beam. Due to the large amounts of data generated and computational demands, this approach would require the development of sophisticated DSP-based data acquisition and processing systems.
3. Modest increases in transmit power and more simple electronic systems could be achieved through moving the pulse generation and power amplifier circuits to the towfish. This would eliminate transmission losses or distortions in the tow-cable. The pulse detector circuit could be eliminated because a trigger signal would be locally available. Only AC power and digital telemetry would need be carried via the tow-cable.
4. Implement two-sided operation so that the useful area of observation for towed surveys could be doubled. This doubles the amount of data produced, requiring more powerful data handling systems on-board the ship.
5. A more mechanically robust tow-body would have to be developed to enable this system to operate under open ocean conditions in adverse weather.

In concert with some or all of the above engineering developments, it is necessary to demonstrate the capabilities and limitations of the IRFS in collaboration with existing survey or test fishing operations. Only by utilizing this new technology in several different environments can the full potential be explored. There are two types of field trials that can be attempted: vessel-based, mobile operations and bottom-mounted, fixed geometry deployments.

Vessel-based operations have the advantages of wide areal coverage and rapid adaptation of the survey to suit location and timing of fish abundance. Figure 9.1 shows a sketch of a possible towed survey geometry utilizing a quad-beam two-sided towed sidescan. Such an operation would be suitable for covering large open waters such as the Strait of Georgia or Johnstone Strait. At 4 knots towing speed, an area greater than 1000 km^2 could be covered in a 10 hour period. In practical terms this means covering the southern Strait of Georgia from Pt. Roberts to Halibut Bank or covering the Canadian portion of Juan de Fuca Strait from Race Rocks to Port Renfrew *in a single day*. A particular advantage of this type of operation is that a second vessel, equipped for echo-sounding or test-fishing, could be directed to investigate targets observed with the long-range beams. This would provide a means of identifying species or stocks, and greatly enhance the efficiency of test-fishery operations. In more confined areas, such as Johnstone Strait, only single-sided operations would be necessary. At 4 knots it would be feasible to survey Johnstone Strait from Kelsey Bay to Port McNeil in a single day, additionally taking advantage of comparisons with the extensive salmon test fisheries conducted by DFO in that area.

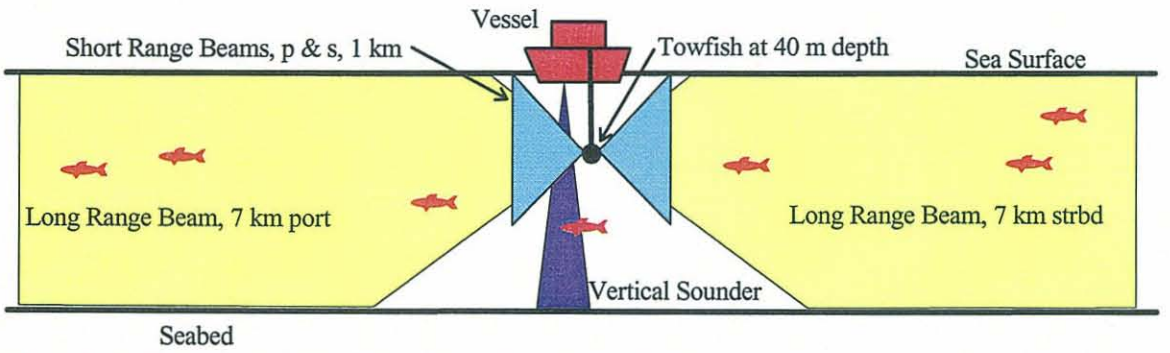

Figure 9.1: Sketch of a proposed towed quad-beam, two-sided swath fisheries sidescan with 14 km total coverage.

The other possible deployment geometry is fixed installations on the seabed, as sketched in Figure 9.2. The advantage of this mode is to provide sustained, 24-hour-a-day surveillance of strategic locations. This is especially effective for migratory species such as salmon. Such a system would provide information on run timing, cross-channel distributions, fish swimming speed, and total abundance. By orienting the beam axis slightly up or down channel, swimming direction can be distinguished by the shape of the echogram traces. Ultimately it would be feasible to automate such systems, so that data is relayed in real-time for distribution to fishery managers. Experience has taught us that the success of such fixed installations is critically dependent on finding the right location. Possible locations might be at the mouth of the Fraser River (near Sandheads), Port Renfrew, Race Rocks, or at some appropriate location in Johnstone Strait. Clearly, the

first steps in such development would be consultation with fishers with local knowledge of fish abundance and behaviour, followed by physical site evaluations. In this geometry, the effects of boundary reverberation can be minimized by removing time-stationary features and looking only for changes against this background. Initial trials of fixed-geometry deployments might utilize a vessel (such as the *Vector*) three-point moored with the sonar lowered on a tripod to the seabed. This approach has the advantage that a number of sites could be evaluated as a prelude to finding a location for a more permanent installation.

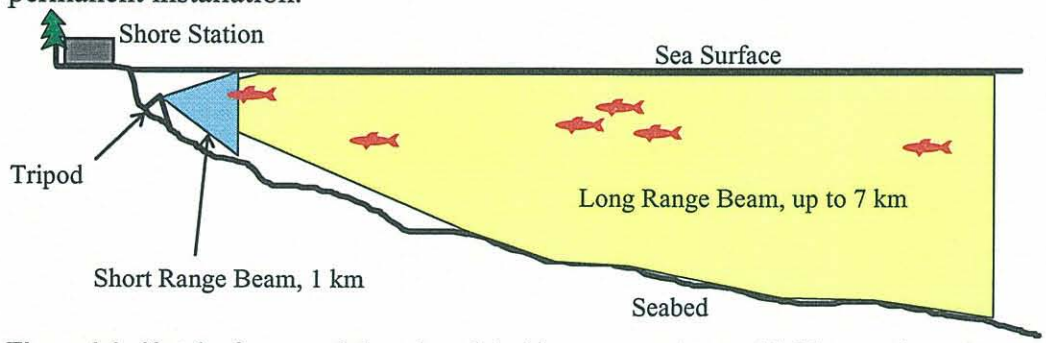

Figure 9.2: Sketch of proposed shore-based dual-beam *acoustic net* with 7 km maximum range.

10. Related Literature:

Bowlin, J., Spiesberger, J., Duda, T., Freitag, L., 1992. Ocean acoustical ray-tracing software RAY, Tech. Rep. WHOI-93-10, Woods Hole Oceanographic Institution, Woods Hole, 49pp.

Clay, C., 1983. Deconvolution of the fish scattering PDF from the echo PDF for single transducer sonar. J. Acoust. Soc. Am. 73, 1989-1994.

Dahl, P. and Mathisen, O., 1983. Measurement of fish target strength and associated directivity at high frequency. *J. Acoust. Soc. Am.* **73**, 1205-1211.

Farmer, D., M. Trevorrow, and B. Pedersen, 1999. Intermediate range fish detection with a 12kHz sidescan sonar, *J. Acoust. Soc. Am.* **106**(5), 2481-2490.

Hewitt, R., Smith, P., and Brown, J., 1976. Development and use of sonar mapping for pelagic stock assessment in the California current area. *Fishery Bull.* **74**(2), 281-300.

Levy, D., Ransom, B., and Burczynski, J., 1991. Hydroacoustic estimation of sockeye salmon abundance and distribution in the Strait of Georgia, 1986, Pacific Salmon Commission Tech. Rep. No. 2, 45pp.

MacLennan, D., 1990. Acoustical measurement of fish abundance. J. Acoust. Soc. Am. 87, 1-15.

Pedersen, B., and M. Trevorrow, 1999. Continuous monitoring of fish in a shallow channel using a fixed horizontal sonar, *J. Acoust. Soc. Am.* **105**(6), 3126-3135.

Quinn, T., and terHart, B., 1987. Movements of adult sockeye salmon (*Oncorhynchus nerka*) in British Columbia coastal waters in relation to temperature and salinity stratification: ultrasonic telemetry results, *Can. Spec. Publ. Fish. Aquat. Sci.* **96**: 61-77.

Revie, J., Weston, D., Harden-Jones, F., and Fox, G., 1990. Identification of fish echoes located at 65 km range by shore-based sonar, *J. Cons. Int. Explor. Mer* **46**: 313-324.

Rusby, J., M. Somers, J. Revie, B. McCartney, and A. Stubbs, 1973. An experimental survey of a herring fishery by long-range sonar, *Marine Biology* **22**: 271-292.

Rusby, J., 1977. Long range survey of a herring fishery by side-scan sonar. *Rapp. P.-V. Reun. Cons. int. Explor. Mer* **170**: 7-14.

Trevorrow, M., and R. Claytor, 1998. Detection of Atlantic herring (*Clupea harengus*) schools in shallow waters using high-frequency sidescan sonars, *Can. J. Fish. Aquat. Sci.* **55**(6), 1419-1429.

Trevorrow, M., 1997. Detection of migratory salmon in the Fraser River using 100kHz sidescan sonars, *Can. J. Fish. Aquat. Sci.* **54**, 1619-1629.

Trevorrow, M., 1998. Boundary scattering limitations to fish detection in shallow water, *Fish. Res.* **35**, 127-135.

Trevorrow, M., 1998. Salmon and herring school detection in shallow waters using sidescan sonars, *Fish. Res.* **35**, 5-14.

Trevorrow, M., 1999. Fish detection in shallow waters using side-looking sonars: the importance of acoustic propagation effects, *Proc. Institute of Acoustics* **21**(9), 101-110.

Trevorrow, M., 2000. An evaluation of a steerable sidescan sonar for surveys of near-surface fish, *Fish Res.* (under review).

Trevorrow, M., 2000. Detection of migratory herring in a shallow channel using 12 and 100 kHz sidescan sonars, *Aquat. Living. Resour.* (under review).

Weston, D., and Revie, J., 1971. Fish echoes on a long-range sonar display, *J. Sound Vib.* **17**(1): 105-112.

Weston, D., and Revie, J., 1989. A 5-day long-range-sonar record of an extensive concentration of fish, *J. Acoust. Soc. Am.* **86**: 1608-1611.

Weston, D., and Andrews, H., 1990. Monthly estimates of fish numbers using a long-range sonar, *J. Cons. Int. Explor. Mer* **47**: 104-111.

Appendix 1: Summary of Operations, *CCGS Vector*, Sept. 4th to 16th, 1998

Date, 1998	Time (PDT)	Action
04 Sept	0930	Loading complete, departed IOS pier
	1100	CTD center of Saanich Inlet (N48° 38.52', W123° 29.68')
	1130 - 1430	Tow tests with IRFS, other system tests and setup
	1500	return to IOS pier
08 Sept.	0600	departed IOS pier headed for Str. of Georgia, towing Grebe
	1245	CTD at GI01 (N48° 58.32', W123° 16.40')
	1411	CTD at GI02 (N49° 02.43', W123° 23.38')
	1534	CTD at VI03 (N49° 06.07', W123° 29.04')
	1700	CTD at VI04 (N49° 12.42', W123° 22.88')
	1800	deployment of WASP (N49° 08.22', W123° 18.16')
	1700	CTD near WASP (N49° 08.28', W123° 18.19')
	1900	arrive, tie-up at W. Vancouver
09 Sept.	0720	departed W. Vancouver, headed for North Arm
	0810	deployed towfish
	0830 - 1112	logging IRFS, sounder, DGPS, Grebe surveys
	1115	CTD near Sandheads (N49° 06.29', W123° 19.93')
	1200 - 1348	continued IRFS, sounder, and Grebe surveys
	1355	CTD near Canoe Pass (N49° 01.47', W123° 15.65')
	1406 - 1507	continued IRFS, sounder, and Grebe surveys, Vector heading W across traffic lanes
	1512	CTD 4 miles off Canoe Pass (N49° 00.33', W123° 20.03')
	1526 - 1744	logging IRFS, sounder, Vector heading NNW 4 miles off
	1806	CTD 4 miles W Sandheads (N49° 06.44', W123° 25.28')
	1818 - 1959	logging IRFS, sounder, Vector heading NNE 4 miles off
	2010	recover towfish
	2012	CTD 4 miles W Airport (N49° 11.47', W123° 23.47')
	2100	dock at W. Vancouver
10 Sept.	0715	depart W. Vancouver, headed for North Arm
	0820	deploy towfish, Grebe conducting surveys nearshore
	0830 - 1205	logging IRFS, sounder, Vector heading South near shore
	1210	CTD near Sandheads (N49° 06.24', W123° 21.13')
	1222 - 1507	continued IRFS, sounder, Grebe surveys, Vector heading W then NNE 2 miles offshore
	1520	recover towfish
	1521	CTD 2 miles W Airport (N49° 13.29', W123° 20.20')
	1600	Vector anchored in 25 m water, W Airport.
	1615	deployed towfish to near bottom
	1634 - 2048	IRFS and sounder logging while Vector at anchor
	1921	CTD at anchor (N49° 13.93', W123° 17.33')
	1800 - 2100	Grebe surveys to W of Vector

	2100	recover towfish
11 Sept.	0700	raising anchor, Grebe begins surveys nearshore
	0728	CTD near Iona Island (N49° 13.84', W123° 17.93')
	0837	CTD near Sandheads (N49° 07.42', W123° 19.42')
	0929	CTD south of Sandheads (N49° 04.31', W123° 19.19')
	1005	CTD near Canoe Pass (N49° 01.54', W123° 15.55')
	1025	deploy towfish, 2 miles offshore Canoe Pass
	1031 - 1556	continued surveys with IRFS, sounder, Grebe nearshore, Vector heading NNW then NNE 2 miles offshore
	1600	recover towfish
	1613	CTD W Pt. Grey (N49° 15.49', W123° 19.69')
	1830	dock at Steveston
12 Sept.	0700	departed Steveston headed for 2 miles off Canoe Pass
	0826	CTD 2 miles off Canoe Pass (N49° 00.63', W123° 18.27')
	0830	deployed towfish, Grebe surveys nearshore working North
	0849 - 0957	logging IRFS, sounder, Vector heading NNW
	1002	CTD 2 miles off Sandheads (N49° 03.32', W123° 22.54')
	1000 - 1500	logging sounder only, IRFS under repair, Vector heading NNE, continued Grebe surveys
	1512	CTD 2 miles W Airport (N49° 09.85', W123° 21.40')
	1620	Grebe departs for Kitsilano base
	1700	CTD near Pt. Grey (N49° 15.77', W123° 19.88')
	1730	crew returns on CCGS Osprey, Vector departs for IOS
	2200	arrive, dock at IOS
14 Sept.	0600	depart IOS, heading for Canoe Pass
	0845	CTD 2 miles W Canoe Pass (N49° 00.71', W123° 18.25')
	0930	deployed towfish
	0952 - 1910	logging IRFS, sounder, heading North 2 miles off
	1520	Vector turns East near Iona Is., then southbound nearshore
	1800 - 1830	test deployments of IMX towfish
	1915	recover IRFS and IMX towfish
	1928	CTD nearshore Sandheads (N49° 03.59', W123° 18.88')
	2000 - 2025	deployment of IMX towfish, Vector heading upriver
	2100	arrive, dock at Steveston
15 Sept.	0700	depart Steveston, heading out to Canoe Pass
	0905	CTD 2 miles W Canoe Pass (N49° 00.49', W123° 18.05')
	0920	deployed IRFS and IMX towfish
	0930 - 1815	logging IRFS, sounder, IMX heading North 2 miles off
	1500	Vector turns East near Iona Is., then southbound nearshore
	1815	recover IRFS and IMX towfish
	1851	CTD Stn. GI02 (N49° 02.58', W123° 23.23')
	1900	Vector heading for Sidney
	2100	pick up additional scientific personnel in Sidney, return to Str. of Georgia

16 Sept.	0600	rendezvous with CCGS Ricker near Westshore Terminals
	0650	deployed IRFS and IMX towfish
	0658 - 0726	logging IRFS, sounder, IMX, Vector heading NNW with Ricker trawl approx. 1 km inshore
	0730 - 0800	recover IRFS and IMX towfish, Vector moves North to Canoe Pass area, redeploy towfish
	0802 - 0848	logging IRFS, sounder, IMX, Vector heading N with Ricker trawl approx. 1.5 km inshore
	0850 - 0920	recover IRFS and IMX towfish, Vector moves North of Sandheads area, redeploy towfish
	0922 - 1005	logging IRFS, sounder, IMX, Vector heading NNE with Ricker trawl approx. 1.5 km inshore
	1010 - 1028	recover IRFS and IMX towfish, Vector moves North to Airport area, redeploy towfish
	1030 - 1105	logging IRFS, sounder, IMX, Vector heading NNE with Ricker trawl approx. 1.5 km inshore
	1112 - 1210	recover IRFS and IMX towfish, Vector moves to position W of Pt. Grey, redeploy towfish
	1214 - 1255	logging IRFS, sounder, IMX, Vector heading W with Ricker trawl approx. 1 km northwards
	1255	recover both towfish
	1307	CTD 4 miles W of Pt. Grey (N49° 15.79', W123° 23.88')
	1410	recover WASP instrument
	1430	Vector heads for IOS
	1800	Vector arrives at IOS, crew disembark

Appendix 2: Summary of CTD casts taken from the *CCGS Vector* during cruise 98-22, Sept. 4th to 16th, 1998

Filename	Date/Time (1998 PDT)	Latitude	Longitude	Depth (m)	Description
98220001	04Sep 1100	N48° 38.52'	W123° 29.68'	125	PatBay
98220002	08Sep 1245	N48° 58.32'	W123° 16.48'	158	Stn GI01
98220003	08Sep 1411	N49° 02.43'	W123° 23.38'	250	Stn GI02
98220004	08Sep 1534	N49° 06.07'	W123° 29.04'	320	Stn VI03
98220005	08Sep 1700	N49° 08.81'	W123° 23.37'	175	Stn VI04
98220006	08Sep 1810	N49° 08.28'	W123° 18.19'	72	1 mi N Sandheads
98220007	09Sep 1115	N49° 06.29'	W123° 19.93'	110	Sandheads N
98220008	09Sep 1355	N49° 01.47'	W123° 15.65'	100	Near Canoe Pass
98220009	09Sep 1512	N49° 00.33'	W123° 20.03'	207	4 mi W Canoe Pass
98220010	09Sep 1806	N49° 06.44'	W123° 25.28'	250	4 mi W Sandheads
98220011	09Sep 2012	N49° 11.47'	W123° 23.47'	260	4 mi W Airport
98220012	10Sep 1210	N49° 06.24'	W123° 21.13'	149	Near Sandheads
98220013	10Sep 1521	N49° 13.29'	W123° 20.20'	194	2 mi W Airport
98220014	10Sep 1921	N49° 13.93'	W123° 17.33'	24	Near Airport
98220015	11Sep 0728	N49° 13.84'	W123° 17.93'	95	Near Iona Is.
98220016	11Sep 0837	N49° 07.42'	W123° 19.42'	100	Sandheads N
98220017	11Sep 0929	N49° 04.31'	W123° 19.19'	102	Sandheads S
98220018	11Sep 1005	N49° 01.54'	W123° 15.55'	96	Near Canoe Pass
98220019	11Sep 1613	N49° 15.49'	W123° 19.69'	180	2 mi W Pt. Grey
98220020	12Sep 0826	N49° 00.63'	W123° 18.27'	180	2 mi W Canoe Pass
98220021	12Sep 1002	N49° 03.32'	W123° 22.54'	244	2 mi W Sandheads
98220022	12Sep 1512	N49° 09.85'	W123° 21.40'	219	2 mi W Airport
98220023	12Sep 1700	N49° 15.77'	W123° 19.88'	177	2 mi W Pt. Grey
98220024	14Sep 0847	N49° 00.71'	W123° 18.25'	181	2 mi W Canoe Pass
98220025	14Sep 1928	N49° 03.59'	W123° 18.88'	120	Sandheads S
98220026	15Sep 0905	N49° 00.49'	W123° 18.05'	179	2 mi W Canoe Pass
98220027	15Sep 1851	N49° 02.58'	W123° 23.23'	250	Stn GI02
98220028	16Sep 1307	N49° 15.79'	W123° 23.88'	200	4 mi W Pt. Grey